



1 **Representing anthropogenic gross land use change, wood harvest and forest**
2 **age dynamics in a global vegetation model ORCHIDEE-MICT (r4259)**

3

4 Chao Yue¹, Philippe Ciais¹, Sebastiaan Luyssaert², Wei Li¹, Matthew J. McGrath¹, Jinfeng Chang³,
5 Shushi Peng⁴

6

7 ¹Laboratoire des Sciences du Climat et de l'Environnement, LSCE/IPSL, CEA-CNRS-UVSQ, Université
8 Paris-Saclay, F-91191 Gif-sur-Yvette, France

9 ²Department of Ecological Sciences, Vrije Universiteit Amsterdam, Amsterdam 1081 HV, The
10 Netherlands,

11 ³Sorbonne Universities (UPMC, Univ Paris 06)-CNRS-IRD-MNHN, LOCEAN/IPSL, 4 place Jussieu,
12 75005 Paris, France

13 ⁴Department of Ecology, College of Urban and Environmental Sciences, Peking University, Beijing
14 100871, China

15

16 *Correspondence to:* Chao Yue (chao.yue@lsce.ipsl.fr)

17

18 **Abstract**

19 Land use change (LUC) is a fundamental anthropogenic disturbance in the global carbon cycle. Here we
20 present model developments in a global dynamic vegetation model ORCHIDEE-MICT for more realistic
21 representation of LUC processes. First, we included gross land use change (primarily shifting cultivation)
22 and forest wood harvest in addition to net land use change. Second, we included sub-grid even-aged land
23 cohorts to represent secondary forests, and to keep track of the age of agricultural lands since LUC, which
24 are associated with variable soil carbon stocks. Combination of these two features allows simulating
25 shifting cultivation with a short rotation length involving mainly secondary forests instead of primary
26 ones. This is in contrast with the traditional approach where a single patch is used for a given land cover
27 type in a model grid cell and forests are thus close to primary ones. We have tested the model over
28 Southern Africa for the period 1501–2005 forced by a historical land use change data set. Including gross
29 land use change and wood harvest has increased LUC emissions in both simulations with (S_{age}) and
30 without ($S_{ageless}$) sub-grid secondary forests, but larger increase is found in $S_{ageless}$ (by a factor of 2) than
31 S_{age} (by a factor of 1.5). Emissions from bi-directional land turnover alone are 35% lower in S_{age} than
32 $S_{ageless}$, mainly because the secondary forests cleared for agricultural land have a lower aboveground
33 biomass than primary ones. We argue that, without representing sub-grid land cohort demography, the



34 additional emissions from land turnover / gross land use change are overestimated. In addition, our
35 developments provide possibilities to account for continental or global forest demographic change
36 resulting from past anthropogenic and natural disturbances.

37

38 Keywords: dynamic vegetation model, gross land use change, age dynamics, shifting cultivation, land use
39 emissions

40

41 **1 Introduction**

42 Land use and land use change (LUC) strongly modifies the properties of the Earth's surface, ecosystem
43 services and their carbon and nutrient fluxes. These activities have significant impacts on the Earth's
44 climate through both biogeochemical and biophysical effects (Foley et al., 2005; Luysaert et al., 2014;
45 Mahmood et al., 2014). When a forest is cleared, the majority of carbon stored in the aboveground
46 biomass is lost as CO₂ to the atmosphere. Such loss can occur within a few years when fire is used in
47 deforestation (Morton et al., 2008), or more slowly through decomposition of the slash left on the ground
48 (Houghton, 1999). Harvested woods for long-term use, though, often take a few decades to degrade
49 (Mason Earles et al., 2012). In addition, LUC changes the balance between litter input and heterotrophic
50 respiration, resulting in changes in soil organic carbon (SOC). A number of meta-analyses (Don et al.,
51 2011; Guo and Gifford, 2002; Poeplau et al., 2011; Powers et al., 2011) have examined SOC change
52 following LUC. Though the directions of SOC change are roughly consistent among typical LUC
53 transitions (e.g., SOC decreases when a forest is converted to cropland; SOC increases when a cropland is
54 converted to pasture), large uncertainties remain regarding the magnitude of SOC changes and its
55 relationship with secondary ecosystem management, climate, soil physical and biogeochemical
56 properties, and the time elapsed since LUC.

57

58 Globally, LUC activities have contributed significantly to historical anthropogenic carbon emissions. It is
59 estimated that about 8 Mkm² of forests were cleared for agricultural purpose and that 20 Mkm² of forests
60 were harvested during 1850–1999, giving rise to cumulative emissions of 124 Pg C, or 33% of the total
61 anthropogenic emissions (Houghton, 1999). Houghton et al. (2012) reviewed LUC emissions from
62 multiple studies and estimated global LUC emissions to be 1.1 Pg C yr⁻¹ for 1980–2009, with an
63 uncertainty of 0.5 Pg C yr⁻¹. Different estimations of historical LUC emissions by Dynamic Global
64 Vegetation Models (DGVM) show a spread as large as 1 Pg C yr⁻¹ (see Fig. 1 in Houghton et al. 2012; see
65 also Hansis et al., 2015 for even larger range among estimations). This is partly due to different forcing
66 data used and initial carbon stocks simulated (Li et al., submitted), but also because of different



67 implementations of LUC processes in dynamic global vegetation models (Prestele et al., 2016). Given the
68 importance of historical LUC emissions and its large uncertainty, a more realistic representation of LUC
69 processes and land management in DGVMs is desirable. This will help improve the diagnostic of the
70 current global carbon cycle perturbation and better forecast its future evolution, which is useful for
71 formulating efficient land-based climate mitigation strategies.

72

73 In most global studies, only net transitions are accounted for in the LUC processes simulated by DGVMs.
74 As such, changes in land use for each model grid cell are diagnosed as the difference in ground fractions
75 of different land cover types between two consecutive years. At a typical spatial resolution of 0.5° for
76 global applications (e.g., TRENDY, Sitch et al., 2015; MsTMIP,
77 http://nacp.ornl.gov/MsTMIP_simulations.shtml), such a scheme ignores the simultaneous transitions of
78 opposite signs between two vegetation types within the same grid cell (i.e., gross transitions). A typical
79 example is shifting cultivation, which involves clearing a forest for a non-permanent cropland. After the
80 cropland is maintained for some time, it is laid fallow to allow forest recovery, and farmers then search
81 for other forests to reinitiate the cycle. Shifting cultivation was historically important in many tropical
82 regions for the subsistence of its inhabitants (Hurtt et al., 2006; Lanly, 1985). Forest management such as
83 clear-cut for wood followed by replanting trees is another type of gross transition. Although it does not
84 entail a change in land cover (forest remaining forest), species choice and forest management can have a
85 significant effect on carbon stocks and fluxes.

86

87 Recently, gross land cover transitions were included in an emulator of the JSBACH DGVM
88 (Wilkenskjeld et al., 2014) and in the LPX-Bern 1.0 DGVM (Stocker et al., 2014). Both studies reported
89 additional LUC carbon emissions when including gross transitions, largely due to the imbalance between
90 moderate carbon uptake in recovering fallow lands and large carbon release from recently cleared lands.
91 Despite promising results of these two studies, among the DGVMs used to assess LUC emissions in the
92 annual update of global carbon budget (Le Quéré et al., 2016), none of them included gross LUC and only
93 a few included wood harvest.

94

95 One must keep in mind, however, that omitting sub-grid gross transitions in DGVMs is largely a scale-
96 dependent issue — suppose DGVMs could run at any finite spatial resolution, then all transitions would
97 be net ones. But given the typical coarse spatial resolution at which DGVMs are often applied, specific
98 routines are needed in the model to include these gross transitions. Another highly relevant aspect is that,
99 DGVMs often use abstract patches associated with certain fractions of a grid cell to represent different
100 land cover types. In most cases only a single patch is used for a certain land cover type. As a result, sub-



101 grid age structure within the same land cover type cannot be represented. When a new forest patch is
102 created due to agricultural abandonment, or re-grows after a clear-cut event, in a DGVM this young forest
103 patch has to be first established and then numerically merged with the existing patch of the same forest
104 type. The carbon stocks are averaged as well, following an area-weighted approach (known as the
105 “dilution approach”). This has an implication for simulated LUC emissions. For example, if shifting
106 cultivation has a rotation cycle of several years to a few decades, the carbon density of the cleared forest
107 will be smaller if a secondary forest is explicitly simulated and cleared, compared to the approach of a
108 single patch representation, where the forest cleared has no age and possibly has high carbon stocks. This
109 calls for inclusion of sub-grid cohorts in DGVMs when simulating gross land use change and forest
110 management. Some recent developments of DGVMs have included this aspect for both forest
111 management and certain LUC processes (Naudts et al., 2015).

112

113 For the reasons described above, the objectives of this manuscript are: (1) to describe the development of
114 a new LUC module, including sub-grid vegetation cohorts, forest harvest and gross land use change in the
115 ORCHIDEE DGVM, that can be run with and without sub-grid age dynamics; (2) to document
116 the model behavior, and (3) to test the hypothesis that including gross transitions and harvest increases the
117 simulated LUC emissions, but that these additional emissions tend to be over-estimated when sub-grid
118 age dynamics are not accounted for.

119 **2 Methods**

120 **2.1 Model developments to include sub-grid vegetation cohorts and gross transitions**

121 **2.1.1 Original land use change module with net transitions only**

122 The model version as the starting point for our development is ORCHIDEE-MICT (r3247), a branch of
123 the ORCHIDEE DGVM (the major version is called the trunk version), the land surface component of
124 the French IPSL Earth System Model (ESM). ORCHIDEE can simulate the energy, water and carbon
125 fluxes between the land surface and the atmosphere. The carbon module simulates vegetation carbon
126 cycle processes, including photosynthesis, photosynthates allocation, vegetation mortality and
127 recruitment, phenology, litter fall and soil carbon decomposition. ORCHIDEE-MICT is a branch initially
128 focusing on improving high-latitude processes (e.g., soil freezing, snow processes, permafrost dynamics
129 and northern wetland) but is now under development to include more processes. Notably, the grassland
130 management module developed in Chang et al. (2013) is included (r2615). This allows for distinction
131 between natural grassland and pasture when simulating historical land use change.

132



133 In ORCHIDEE, land cover types are represented as plant function types (PFTs), with each PFT being
134 associated with a set of parameters. A typical model simulation consists of two stages: a spin-up stage
135 with stable or constant forcing data, where the model is run until an approximately equilibrium state is
136 reached, to mimic an era with no appreciable human perturbation, and a transient stage, where the model
137 is forced with temporally varying forcings (e.g., climate, atmospheric CO₂, land cover etc.). The land use
138 change module prior to this study accounts for net transitions only (Piao et al., 2009a) and has been used
139 in many applications (e.g., CMIP5, <http://icmc.ipsl.fr/index.php/cmip5>; TRENDY, Sitch et al., 2015). To
140 simulate historical land use change, a spin-up stage is started with a given initial land cover map (i.e., a
141 PFT map), and then vegetation distribution is updated annually with prescribed PFT map time series
142 during the transient simulation. The LUC module simply compares grid cell fractions of different PFTs
143 between the current simulation year and the next year. Then twelve vegetative PFTs (all standard model
144 PFTs excluding the bare soil PFT) are separated into two groups with expanding versus contracting areas.
145 Carbon stocks and associated carbon fluxes on shrinking PFTs are displaced to expanding PFTs in
146 proportion to their respective surface increments.

147 **2.1.2 Concept of gross transitions in relation to vegetation age structure**

148 The numerical implementation of net transitions is straightforward. However, as explained in the
149 introduction, this scheme omits important sub-grid gross land use transitions. Figure 1 uses an exemplary
150 grid cell to illustrate the difference between the two LUC schemes: one accounting for net transitions only
151 (Fig. 1b), and the other accounting for gross transitions but with no sub-grid cohorts (Fig. 1c & 1d).
152 Although the areas of forest and cropland after LUC are identical (Fig. 1b & 1d), carbon stocks for the
153 same vegetation type (e.g., forest) are different between the two schemes. According to the net transition
154 scheme, the carbon stock of the final forest patch shown in Fig. 1b remains intact. But under the gross
155 scheme (Fig. 1d), the post-LUC forest carbon stock is an area-weighted mean between the original forest
156 patch not impacted by LUC, and the newly established forest with a low carbon density that results from
157 cropland abandonment. Consequently the carbon stock of the grid cell is expected to be smaller in Fig. 1d
158 than in 1b. LUC carbon emission in Fig 1d is conversely larger than in 1b.

159

160 Figure 1c represents the real land cover state after LUC, while the dilution shown in Fig. 1d is only a
161 necessary simplification when no sub-grid cohorts are represented in the model. Ideally, the model
162 capacity could be expanded to include cohorts, to represent the real world case as in Fig. 1c. In addition,
163 inclusion of sub-grid cohorts would allow not only the distinction between original intact forest and
164 newly established forest, but also allow distinguishing among different forest cohorts (e.g., primary
165 versus secondary forests) regarding the decision on which forest should be cleared for cropland.

166



167 Figure 2 illustrates a case where gross LUC is combined with sub-grid cohort representation in the model,
168 which allows accommodating land use transitions in a more realistic way. Here, multiple patches within a
169 grid cell are used to represent cohorts of a single vegetation type but with different ages since
170 establishment. These cohorts often have different carbon stocks either due to different lengths in carbon
171 accumulation time (e.g., for forest) or due to different extents to which the legacy soil carbon is reserved
172 (e.g., for cropland establishing on former forest). The areas subject to gross LUC transition in Fig. 2a &
173 2b remain the same as in Fig. 1a (dashed red rectangles), but primary and secondary forests are cleared in
174 Fig. 2a and Fig. 2b, respectively. Thus LUC emissions from clearing of primary forest are expected to be
175 higher due to its higher biomass stock. Correspondingly, the legacy soil carbon stocks on the cohort of
176 new cropland are also higher (shown in Fig. 2b & 2d).

177

178 Figure 1 and Fig. 2 have shown the example of LUC transitions between forest and cropland, but other
179 types of land use changes, including forest harvest, can be handled in a similar way. In the case of forest
180 harvest, such as in Fig. 2, having cohorts avoids the simplification to merge a young re-established forest
181 after harvest with the original forest, which serves as the exact source of harvest. This can effectively
182 simulate forest management practices inducing rotations between different forest cohorts that vary with
183 time (e.g., see McGrath et al., 2015 for forest management history in Europe).

184 2.1.3 Expansion of ORCHIDEE-MICT capacity to represent sub-grid vegetation cohorts

185 In order to simulate gross LUC combined with sub-grid vegetation cohorts as illustrated in Fig. 2, we
186 expanded the ORCHIDEE-MICT capability to include sub-grid even-aged cohorts. This necessitates
187 multiple patches within a grid cell for a single PFT, which inherit most of the parameters from their
188 parent PFT (they still belong to the same PFT and thus are largely physically similar). These patches are
189 named here *Cohort Functional Types (CFT)*, to be distinguished from the original *plant functional types*.
190 In this sense, the original PFTs actually become “meta-PFTs” which we label as meta-classes (MTCs). As
191 subsequent land use changes greatly increase the total number of CFTs, the computational demand will be
192 greatly increased. Hence, the number of CFTs within an MTC is limited to a user-defined number.

193

194 ORCHIDEE-trunk has a feature called “PFT externalization” which allows creating a user-specified new
195 PFT by inheriting its parameters from an existing one whose parameterization is well defined. A user can
196 then modify specific parameters at their convenience. Based on this feature, the ORCHIDEE-CAN (svn
197 rev. = r2566; Naudts et al., 2015, Page 2037) branch incorporated representation of sub-grid forest age
198 classes (i.e., equivalent to our CFTs here) for European forests. Each forest age class is an inheritance of a
199 given forest MTC. There, forest age classes were defined by different tree diameters. When a forest of a
200 certain age class reaches its diameter limit, it moves into the next age class, and is merged with the



201 existing forest patch if there is one. All associated biophysical and biogeochemical variables are merged
202 as well following an area-weighted mean approach.

203

204 ORCHIDEE-MICT also inherits this “externalization” feature from ORCHIDEE-trunk. Here we ported
205 the codes of forest age class functionality from ORCHIDEE-CAN, and made all necessary adaptations into
206 ORCHIDEE-MICT, to develop the CFT functionality needed for LUC simulation with cohorts. Forest
207 canopy structure and tree diameters are simulated in ORCHIDEE-CAN, using an allometry-based
208 allocation scheme (based on the pipe model) and a tree-height dependent light attenuation scheme
209 (Naudts et al., 2015, Page 2038). ORCHIDEE-MICT, however, uses the same big-leaf approximation and
210 exponential attenuation of light in the canopy as in ORCHIDEE-trunk to scale photosynthesis from leaf to
211 canopy depth (Krinner et al., 2005). As a result, no tree diameter classes exist in ORCHIDEE-MICT and
212 we thus use forest woody biomass to delimit different cohorts, with older cohorts having a higher woody
213 biomass. In addition, we expanded the concept of CFT to croplands, natural grasslands and pastures.
214 Cohorts are defined with their soil carbon stocks for these herbaceous vegetation types; this is a definition
215 relevant to LUC emission calculation. For these short-vegetation CFTs, we assume that the older their age
216 since LUC disturbance, the lower their soil carbon will be (assuming a typical case of cropland
217 originating from forest). The biomass or soil carbon thresholds that delineate different CFTs must be
218 properly parameterized in order to have sensible CFT segregation within different contexts of land use
219 change. This will be further detailed in the Sect 2.2.3. In practice, for single-site simulation, the
220 parameterization could be set up via a configuration file enumerating the thresholds for all CFTs. For
221 regional applications, an input file containing thresholds for each grid cell will be used.

222

223 The implementation of sub-grid cohort function types as inheritances of meta-classes and the
224 corresponding hierarchy are exhibited in Fig. 3a. “Tier 1” of the “*Model parameterization hierarchy*”
225 corresponds to the four basic vegetation types (forest, natural grassland, pasture, and croplands,
226 abbreviated as *f*, *g*, *p*, *c* respectively). “Tier 2” corresponds to meta-classes in ORCHIDEE-MICT, which
227 contain one bare soil MTC and fourteen vegetative MTCs, with each vegetative MTC belonging to one of
228 the four basic vegetation types. “Tier 3” corresponds to cohort function types. A cohort functional type is
229 conveniently noted as CFT_{ij} to denote that it inherits its parameter values from the MTC_i and belongs to
230 the j^{th} cohort. Forest MTCs contain six CFTs and herbaceous MTCs contain two CFTs. The number of
231 CFTs for each MTC is not hard-coded in the model and can be specified by users via a configuration file.

232

233 With sub-grid cohorts, the model spin-up run is initiated with an input MTC map, essentially the same as
234 in the case without sub-grid cohorts (recall that in Sect. 2.1.1 this MTC map is called a PFT map). But the



235 difference is that the initial prescribed areas (as fractions of grid cell area) of different MTCs are assigned
236 to their youngest cohorts. With model spin-up going on, forest woody mass will grow to exceed the
237 thresholds of the first cohort, so that forests will move to the second cohort, and so on. At the end of spin-
238 up, all forests thus end up in the oldest cohort of each MTC. The same case applies to herbaceous MTCs,
239 given that cohort thresholds are properly defined.

240

241 Natural forest mortality in ORCHIDEE could be either prescribed as a constant rate or dynamically
242 simulated, but the mortality process only has an effect to reduce the amount of existing biomass in each
243 forest cohort, when dead biomass is moved to litter pool and recruitment carbon stocks are integrated.
244 This remains the same as the case without sub-grid cohorts, i.e., natural recruitments do not create young
245 cohorts but just “dilute” the carbon stock of each forest cohort. Open vegetation fires are handled in a
246 similar manner. ORCHIDEE-MICT has integrated a prognostic fire module (Yue et al., 2014) to simulate
247 open grassland and forest fires arising from both natural and anthropogenic ignitions. Fire-induced forest
248 mortality is handled similarly as natural mortality, i.e., fire-induced recruitments lead to no young cohort
249 creation but just reduce the existing carbon stock. Other forest disturbances, such as wind-throw, diseases
250 and insect outbreaks, are not explicitly considered. Because of these reasons, after the spin-up, the only
251 way to create secondary cohorts is through land use change.

252

253 When entering transient simulations with land use change being included, younger cohorts will begin to
254 be created as a result of different LUC activities. From a modeling perspective, the oldest cohorts in
255 ORCHIDEE-MICT are somewhat equivalent to the primary lands (especially, the oldest forest cohorts
256 are equivalent to primary forests), and other younger cohorts are analogue to secondary lands.

257 **2.1.4 Model developments to include gross land use change and forest harvest, with and without** 258 **sub-grid cohorts**

259 This section describes the implementation of gross land use change and forest harvest with sub-grid
260 CFTs. We focus on the implementation with sub-grid cohorts, because the same LUC process without
261 cohorts could be simply treated as a particular case where all MTCs have only one single cohort. The
262 module interface is designed to receive forcing information on land area fluxes among four basic land
263 cover types of forest (f), natural grassland (g), pasture (p) and cropland (c), taking into account the current
264 LUC modeling landscape in DGVMs (as briefly reviewed in the Introduction) and the availability of land-
265 use change history reconstructions (e.g., Hurtt et al., 2011). In order to compare the simulation results
266 from the gross LUC module with the original net-transition-only LUC module, we separate the gross
267 LUC areas into two additive terms: ‘net change’ equivalent to the original net transition (prescribed by the
268 matrix M_{net}), and ‘land turnover’ for the bi-directional equal land fluxes between any pair of land cover



269 types (prescribed by the matrix M_{turnover}). Similarly, the forest harvest information is prescribed in a third
 270 matrix M_{harvest} . For the moment, information for all the three LUC types is provided as fraction of grid cell
 271 area. This is a deliberate choice, mainly for the convenience of progressive stage-wise model
 272 development. We will come back to the influence of this choice within the land use decision contexts in
 273 the Discussion section.

274

275 The key processes of the gross LUC module with CFTs are shown in Fig. 4, comprising in total 6 steps.
 276 The LUC module is called at the first day of each year. Input data are the three matrices. M_{net} and M_{turnover}
 277 are both square matrices with a size of 4 by 4:

$$\mathbf{M}_{\text{net}} (\mathbf{M}_{\text{turnover}}) = \begin{array}{c} \text{Donating land type} \\ \left[\begin{array}{c} \text{forest} \\ \text{grassland} \\ \text{pasture} \\ \text{cropland} \end{array} \right] \begin{array}{c} \text{Receiving land type} \\ \left[\begin{array}{cccc} \text{forest} & \text{grassland} & \text{pasture} & \text{cropland} \\ F_{f \triangleright f} & F_{f \triangleright g} & F_{f \triangleright p} & F_{f \triangleright c} \\ F_{g \triangleright f} & F_{g \triangleright g} & F_{g \triangleright p} & F_{g \triangleright c} \\ F_{p \triangleright f} & F_{p \triangleright g} & F_{p \triangleright p} & F_{p \triangleright c} \\ F_{c \triangleright f} & F_{c \triangleright g} & F_{c \triangleright p} & F_{c \triangleright c} \end{array} \right] \end{array} \right] \end{array} \quad \text{Eq (1)}$$

278

279 Where the element $F_{i \triangleright j}$ denotes the land flux from land cover type i to j , with i, j being elements of the
 280 vector of $[f \ g \ p \ c]^T$. The diagonal elements correspond to land area intact from any land use transitions
 281 and are simply ignored in the LUC module. By definition, M_{turnover} is a symmetric square matrix. M_{harvest} is
 282 a matrix with only two elements: harvest area from primary and secondary harvest.

283

284 As explained in Sect. 2.1.3, the construction of CFTs within the model follows the “model
 285 parameterization hierarchy” shown in Fig. 3a. The cohort age subjected to LUC of is one of the most
 286 important considerations in land use change decisions, especially in the context of land turnover and
 287 forest harvest. This necessitates a re-organization of the CFTs to derive the “LUC hierarchy” shown in
 288 Fig. 3b, where Tier 2 information is about areas of different cohorts of the same land cover type, and Tier
 289 3 remains on the level of CFTs. So the Step 1 in the LUC module (Fig. 4) is to construct the “LUC
 290 hierarchy”, i.e., to calculate within the model the areas of each cohort for each vegetation type.

291

292 When implementing LUC matrices, all information of land transitions between the four basic land cover
 293 types must first be downscaled on the cohort tier (i.e., decision on which cohort is subjected to LUC) and
 294 then on the CFT tier (i.e., how LUC-affected area is distributed among different comprising meta-classes
 295 within each cohort, refer also to Fig. 3b). This is achieved in Step 2 as shown in Fig. 4. Because all the
 296 newly established lands, regardless of their originating LUC process, must belong to the youngest CFT of



297 the MTCs that comprise the target land cover type, the ultimate outcome of Step 2 is a single (large)
 298 matrix $\mathbf{M}_{n\text{CFT}, n\text{MTC}}$ ($n\text{CFT} = \#$ of CFTs, $n\text{MTC} = \#$ of MTCs), which indicates the area transferred from
 299 each CFT to the youngest cohort of the concerning MTC. The rules to convert LUC matrices into
 300 components of $\mathbf{M}_{n\text{CFT}, n\text{MTC}}$ depend on LUC types and will be explained in detail later. But as long as Step
 301 2 is done, the remaining steps are rather straightforward.

302

303 Step 3 handles forest wood collection (here ‘collection’ rather than ‘harvest’ is used, to avoid the
 304 confusion with forest wood harvest which is a means of forest management), from forest being converted
 305 to other land cover types, and forestry harvest (forest remaining forest). We assume that a certain fraction
 306 of aboveground woody biomass (i.e., sapwood and heartwood) is lost as instant CO_2 flux into the
 307 atmosphere (i.e., due to on-site disturbance), and that the remaining wood is collected as wood product
 308 pools. Step 4 involves the proper displacement of associated carbon stocks and fluxes from the donating
 309 CFTs to the newly established (youngest) cohorts of MTCs, after wood collection. Notably, the legacy
 310 carbon stocks in litter and soil are collected from the donating CFTs and transferred to the newly
 311 established youngest CFTs. Then in Step 5, each youngest CFT cohort is established and initialized, with
 312 its fraction of grid-cell area being the sum of contributed areas given by each source CFT. Finally, in Step
 313 6, a newly established cohort is merged with the existing youngest CFT cohort if there is already one.
 314 When merging of stocks or fluxes between the newly established and existing CFTs, an area-weighted
 315 mean approach is followed:

$$316 \quad x_{merged} = \frac{x_{new} \times area_{new} + x_{existing} \times area_{existing}}{area_{new} + area_{existing}} \quad \text{Eq (2)}$$

317 Where x is the variable in question (e.g., leaf biomass, soil carbon stock etc.), x_{new} and $x_{existing}$ are the
 318 values of the newly established patch and existing patch before merging and x_{merged} is the value of the
 319 generated patch after merging. $area_{new}$ and $area_{existing}$ are patch areas of the newly established and
 320 existing patches, respectively.

321

322 We now return to Step 2, explaining the different rules used to build the $\mathbf{M}_{n\text{CFT}, n\text{MTC}}$ components for
 323 different LUC types. We start with $\mathbf{M}_{harvest}$ by assuming that it precedes conversion of forest to other land
 324 cover types (i.e., land turnover or net land use change). As is explained, the LUC module is designed to
 325 receive externally prescribed harvest information, especially from the widely used LUH1 reconstruction
 326 (Hurtt et al., 2011), rather than to determine harvest volume internally within in the model, which is very
 327 different from ORCHIDEE-CAN. The LUH data makes distinction between harvests from primary and
 328 secondary forests. The harvest information is provided as both forest area and wood volume. Here we
 329 used the area information (again a deliberate choice which will be discussed in Sect. 4). Because of this,



330 ensuring the consistency between the harvest area in the forcing and that being actually realized in the
331 model is an important consideration. Moreover, as we want to compare simulated LUC impacts between
332 the two model configurations with and without sub-grid cohorts, it is necessary to ensure that exactly the
333 same LUC area is realized in both configurations. This involves a set of decision rules to properly allocate
334 the prescribed harvest area into different forest cohorts.

335

336 Implementation of primary forest harvest is straightforward: we always start with the oldest cohort and
337 move sequentially downwards to younger ones if older cohorts are exhausted, until the prescribed harvest
338 demand is fulfilled. For secondary forest harvest, we start with intermediate-aged cohorts. But if the
339 existing area of intermediate-aged cohorts is not sufficient to fulfill the prescribed harvest area, we are left
340 with two options to either search upwards for older cohorts or downwards for younger ones. We decide to
341 first go first for upward searching and then for downward searching, if all cohorts older than intermediate
342 age still cannot fulfill the prescribed harvest demand. This rule allows potential temporal changes in
343 harvested area to be accommodated, as explained in Fig. 5. Under such a scheme, (1) at the very
344 beginning (after spin-up) and before the existence of any secondary forests, harvest will start with the
345 oldest cohort, i.e., corresponding to harvest of primary forests (sometimes, because of the inconsistency
346 between the input harvest information and existing forest cohort structure in the model, “secondary”
347 forest harvest could be prescribed for pixels where only primary forests exist in the model). (2) If harvest
348 area of secondary forest remains stable, then as soon as sufficient intermediate-aged cohorts are created
349 via conversion of primary forest to re-growing younger cohorts, a corresponding stable cycle would be
350 maintained in the model as well. (3) If the harvest area increases, the upward searching would allow
351 additional harvest of primary forests (i.e., area subject to the stable rotation cycle is expanded). (4) If the
352 harvest area decreases, the moving of cohorts from younger to older ones independent of any LUC
353 activities would allow restoring older cohorts— e.g. a consequence of abandonment of forest
354 management. (5) Finally, the downward searching for younger cohorts after exhausting all other older
355 cohorts is solely to ensure the consistency between prescribed input harvest area and that actually realized
356 in the model. Hence, this scheme is designed in order to faithfully implement the prescribed harvest areas
357 in the model explicitly considering the forest successional states (i.e., primary or secondary). But when
358 this is not possible because of inevitable disagreement between the model and forcing data, harvest areas
359 of primary and secondary forests could mutually compensate for each other in the model, to ensure the
360 their prescribed total harvest area is till realized.

361

362 A number of studies reported that fallow lengths for shifting cultivation could range from a few years to
363 more than 50 years depending on different regions, with the majority being 10–40 years (Bruun et al.,



364 2006; Mertz et al., 2008; Thrupp et al., 1997; van Vliet et al., 2012), and there is tendency in reduction of
365 fallow lengths possibly because of increased population pressure (van Vliet et al., 2012). Hurtt et al.
366 (2006) assumed a mean residence time of 15 years for shifting cultivation for tropical regions in the
367 LUH1 reconstruction data. Based on these evidences, we assume forest clearance for shifting cultivation
368 to occur primarily in secondary forests, and treat it similarly as secondary forest harvest when allocating
369 the prescribed LUC area into different cohorts. The only difference is that the destination land cover
370 remains forest in the case of forest harvest but is agricultural land in the case of shifting cultivation. For
371 all other land transfers in shifting cultivation (e.g., pasture to forest), we start exclusively from the oldest
372 cohort and move downwards to younger ones. For net land use change, priority is again given to older
373 cohorts followed by younger ones.

374

375 Finally, we still need to downscale the LUC area in each cohort to its component CFTs. This is done by
376 allocating the LUC area in each cohort to its member CFTs in proportion to the existing area of each CFT.

377 **2.1.5 LUC processes that remain unchanged in the model**

378 ORCHIDEE simulates two wood product pools with turnover times of 10 years and 100 years,
379 respectively. Fractions of aboveground woody biomass as instant on-site loss (F_{instant}), and entering into
380 the two wood product pools ($F_{10\text{yr}}$, $F_{100\text{yr}}$) follow the values in the original net-transition-only LUC scheme
381 (Piao et al., 2009a), as shown in Table 1. Other biomass compartments (i.e., leaves, fine roots, coarse
382 roots, fruits and reserve pool) are transferred to litter pools during forest harvest or deforestation.

383

384 Other processes relevant to LUC are left unchanged from the original model version. In particular, crop
385 harvest is applied to cropland CFTs with 45% of biomass turnover being ‘harvested’ in the model and
386 exported outside the ecosystem (Piao et al., 2009a). Pasture CFTs are also harvested in the same fashion.
387 Fires are simulated with a prognostic module, but as explained in Sect. 2.1.3, fire disturbances do not lead
388 to creation of young cohorts, but only their carbon consequences (e.g., emissions, vegetation mortality,
389 etc.) are included.

390 **2.2 Simulation set-up**

391 **2.2.1 Definition of land-use change emissions (E_{LUC}) and carbon flux sign convention**

392 The land carbon balance simulated by ORCHIDEE r4259 (i.e., net biome production or NBP), when land
393 use change is included, is defined as:

394

$$395 \text{NBP} = \text{NPP} + F_{\text{Inst}} + F_{\text{Wood}} + F_{\text{HR}} + F_{\text{Fire}} + F_{\text{AH}} + F_{\text{Pasture}} \quad \text{Eq (3)}$$

396



397 Where NPP is the net primary production, and all fluxes with “F” notation are outward carbon fluxes
398 from the land system (they are assigned a negative sign following the ecosystem convention, indicating
399 that carbon is lost from ecosystems), with F_{Inst} for the instantaneous carbon flux during LUC (e.g., carbon
400 release arising from site preparation, land-clearing burning etc.), F_{Wood} for the delayed carbon release due
401 to wood products degradation, F_{HR} for heterotrophic respiration from litter and soil organic carbon, and
402 F_{AH} for agricultural harvest on both croplands and pastures (assumed to be released to the atmosphere
403 within one year), and F_{Pasture} for carbon sources from pastures than harvest, i.e., export of animal
404 production and methane emissions (see Chang et al., 2015 for details).

405

406 The LUC emissions (E_{LUC}) are quantified as the difference in simulated NBP between two paired
407 simulations, with LUC (or a specific LUC process) included in one simulation but not the other one:

408

$$409 \quad E_{\text{LUC}} = \text{NBP}_{\text{LUC}} - \text{NBP}_{\text{control}} \quad \text{Eq (4)}$$

410

411 Where, NBP_{LUC} and $\text{NBP}_{\text{control}}$ are NBP simulated with and without LUC. A negative E_{LUC} denotes a
412 carbon source to the atmosphere, i.e., ecosystem carbon sink is reduced because of land use change. This
413 definition follows Pongratz et al. (2014, Page 178) and is also the same as used in TRENDY (Sitch et al.,
414 2015) simulations and Le Quéré et al. (2016). As explained by Pongratz et al. (2014), such a definition
415 quantifies the “net” LUC flux because it integrates both emissions to the atmosphere (e.g., deforestation)
416 and uptakes by potentially recovering vegetation (e.g., agricultural abandonment). More specifically, this
417 corresponds to the definition “D3” using uncoupled DGVM simulations in Pongratz et al. (2014, Eq. 15c,
418 Page 187), which contains instantaneous fluxes, legacy fluxes, and “loss of additional sink (source)
419 capacity (LOAS)”.

420

421 Instantaneous fluxes refer to the carbon emissions directly arising from LUC, often occurring within the
422 first year since LUC (F_{Inst} in our case). Legacy fluxes arise from the readjustment of carbon stocks to the
423 new type of vegetation and/or type and intensity of management over time (Pongratz et al., 2014), and
424 “loss of additional sink (source) capacity (LOAS)” refers to the carbon sink/source difference between the
425 actual land cover after LUC and the otherwise potential one under environmental perturbations. All other
426 flux terms on the right side of Eq. (3) except F_{Inst} contribute to the legacy fluxes and LOAS. Here, as our
427 model development mainly distinguishes the biomass carbon of secondary forests and it’s thus expected
428 that F_{Inst} and F_{Wood} will be the major fluxes to have influence on simulated E_{LUC} . To facilitate the
429 demonstration of model behaviour, we refer to F_{Inst} and F_{Wood} collectively to as “LUC-associated direct
430 fluxes” and their variations will be examined in detail on using an idealized grid cell simulation.



431

432 The model developments presented here enable us to make two parallel simulations that include LUC:
433 with and without sub-grid age dynamics. Their simulated E_{LUC} can thus be compared, to separate the
434 effect of including sub-grid age dynamics. Henceforth for brevity, we denote the simulation without
435 sub-grid age dynamics as $S_{ageless}$, and the one with age dynamics as S_{age} .

436 2.2.2 Idealized simulation on a single grid cell

437 We conducted an idealized grid cell simulation with prescribed land cover and LUC matrices, to compare
438 in detail the simulated carbon pools and fluxes between S_{age} and $S_{ageless}$. The geographical coordinates of
439 the simulation site are 9.25°S, 18.25°E at a 0.5° global grid, in the north of Angola, Africa, where the
440 miombo woodlands are known to be subject to practices of shifting cultivation. The ESA CCI land cover
441 map for the 5-year period of 2003–2007 (<https://www.esa-landcover-cci.org/>) shows a dominant fraction
442 of tropical deciduous broadleaf forest for this grid cell. Hence for this idealized experiment, the initial
443 vegetation composition is prescribed as 85% of tropical deciduous broadleaf forest and 15% of C4
444 cropland. As we will focus on the LUC impacts, other model forcings (climate, atmospheric CO₂, etc.) are
445 held as constant, with climate input data recycling the year of 1901 (CRUNCEP-v5.3.2 climate data,
446 <https://esgf.extra.cea.fr/thredds/fileServer/store/p529viov/cruncep/readme.html>) and atmospheric CO₂
447 concentration being fixed at 350 ppm. The model is tested for a hypothesize scenario of constant annual
448 land turnover with 5% of grid cell area between forest and C4 cropland. Forest harvest of the same
449 intensity is expected to have largely similar impact. The spin-up was run for 450 years until biomass and
450 soil C stocks reached equilibrium and the mean annual net biome production (NBP) was close to zero.
451 Starting from the spin-up, a transient simulation with the prescribed LUC matrix was performed for 100
452 years.

453 2.2.3 Simulation over Southern Africa

454 Subsequently, the model behavior has been documented for a real-world case over the region of Southern
455 Africa (south to the equator of the African continent). All three LUC types occurred historically in this
456 region, making it ideal to demonstrate model behavior especially regarding forest cohort dynamics as
457 presented in Fig. 5. This regional simulation serves a single purpose — to further exemplify model
458 features that cannot be sufficiently demonstrated on one grid cell.

459

460 The regional simulation is done at 2° resolution for 1501–2005. We used land use reconstruction from
461 LUH1 covering 1501–2013 (Hurt et al., 2011, http://luh.umd.edu/data.shtml#LUH1_Data) re-gridded
462 from the original 0.5° to a 2° spatial resolution. We derived from the LUH1 dataset the matrices of the
463 three types of land use change: net land use change, land turnover and wood harvest. Land turnover



464 information is extracted from LUH1 as the minimum land fluxes between two vegetation types. Because
465 all LUC activities are represented with matrices, strict area conservation is ensured when re-gridding a
466 matrix from a higher to lower spatial resolution. Climate forcing data are from CRUNCEP-v5.3.2 at a 2°
467 resolution. For the spin-up, climate data were cycled from 1901 to 1910, with atmospheric CO₂
468 concentration fixed at 1750 level (277 ppm). In the transient simulation, atmospheric CO₂ concentration
469 began to increase in 1750, climate data were varied starting 1901. The dynamic vegetation module was
470 turned off, in order to apply the prescribed historical land use change. Factorial simulations are conducted
471 to quantify E_{LUC} from each of the three LUC types, as shown in Table 2.

472

473 Each forest MTC has six CFTs to represent six cohorts. The woody mass thresholds are set in a way that
474 they correspond roughly to the woody masses at ages of 3, 9, 15, 30, 50 years, and the mature or primary
475 forest during the spin-up simulation, respectively, for Cohort₁ to Cohort₆. The Cohort₃ with an age of 15
476 years is the primary target for secondary forest harvest and land turnover (or shifting cultivation),
477 corresponding to the mean residence time of 15 years of shifting cultivation assumed in LUH1 (Hurtt et
478 al., 2006) data. We set two CFTs for each herbaceous MTC with a high and low soil carbon density,
479 respectively. The CFT thresholds of soil carbon stock are the same for all herbaceous MTCs. We first
480 calculate the maximum soil carbon stock of all MTCs (including the forest ones) at the end of spin-up for
481 each grid cell, and cohort thresholds are then taken as this maximum value and its 65% value. Because the
482 energy balance in ORCHIDEE-MICT is resolved for the average of all CFTs over a grid cell, and the
483 hydrological balance is resolved for three sub-grid water columns (i.e. the water column of bare soil,
484 forest and herbaceous vegetation), we expect the factors influencing soil carbon decomposition (e.g., soil
485 temperature, soil moisture) to have little variation among CFTs of the same MTC. This justifies the small
486 number of herbaceous CFTs, for the sake of computation efficiency.

487 3 Results

488 3.1 Grid cell simulations with and without sub-grid forest age dynamics

489 3.1.1 Temporal patterns of biomass carbon stock during the spin-up and transient simulations

490 Figure 6a and 6b exhibit the evolution of above- and belowground biomass for both S_{ageless} and S_{age}
491 simulations, for the spin-up and transient simulation for a test grid cell located in Angola. For this test an
492 annual forest-cropland turnover of 5% of the grid cell area was imposed. Figure 6c shows changes in the
493 ground fractional cover of different forest cohorts in S_{age} during the transient simulation. S_{ageless} and S_{age}
494 share the same biomass accretion with time during the spin-up, but S_{age} shows a succession of forest
495 cohorts — with biomass moving from one cohort to the next (Fig. 6a & 6b). At the end of the spin-up, all
496 biomass is found in Cohort₆ (i.e., the oldest cohort) in S_{age}, with an initial forest cover of 85%.



497

498 More differences emerge when entering the transient simulation. Aboveground biomass in S_{ageless} shows
499 an initial sharp drop followed by a more gradual decline under constant land turnover, because biomass of
500 the single forest patch is constantly ‘diluted’ by merging with the new forest patch with a low biomass,
501 which is established out of land turnover (see also Fig. 1). Belowground biomass, however, shows a
502 corresponding initial drop but then slightly increases. Eventually, both above- and belowground biomass
503 stocks in S_{ageless} reach a new equilibrium, which are lower than their values at the end of the spin-up. By
504 contrast, in S_{age} , the fraction of Cohort_6 declines with the start of the transient simulation because of
505 conversion to cropland. This decline continues until the 12th year, after which the remaining Cohort_6
506 covers only 30% of the grid cell (Fig. 6h). Younger cohorts are progressively created as forests restore
507 after shifting agriculture abandonment, with the Cohort_1 (i.e., the youngest one) appearing during the
508 initial 6 years after the start of LUC, after which its biomass is moved into Cohort_2 (Fig. 6c & 6d).
509 Cohort_3 starts to appear at the 12th year when biomass in Cohort_2 moves into it. Then its coverage declines
510 as this cohort, rather than Cohort_6 , is used as the source for shifting cropland, according to the model rule
511 that secondary forest is taken prior to primary forest in the land turnover (Fig. 5). After the initial 15 years
512 (the rough age of Cohort_3), the fractions of Cohort_1 , Cohort_2 and Cohort_3 reach a dynamic stable state.
513

514 While the aboveground biomass continuously grows during the spin-up, the belowground biomass first
515 increases with time and then slightly declines before reaching the equilibrium value. This is because
516 ORCHIDEE-MICT has a preferential allocation of NPP allocation to belowground sapwood when forests
517 are young. The small decline in belowground biomass in the late spin-up stage thus results from an almost
518 stabilized NPP (under a big-leaf approximation), the reduced belowground allocation and a constant
519 mortality. Because of this feature, ORCHIDEE-MICT creates a higher belowground biomass in younger
520 forest cohorts (e.g., Cohort_2 and Cohort_3 in Fig. 6a & 6b) in S_{age} than the single forest patch in S_{ageless} in
521 the transient simulation. However, the aboveground biomass in younger Cohort_2 and Cohort_3 in S_{age} is
522 lower than S_{ageless} . The difference in biomass influences the simulated E_{LUC} between these two
523 simulations, as we will discuss in detail later.

524 3.1.2 LUC-associated direct carbon fluxes

525 As shown in Fig. 7a, in S_{ageless} , the instantaneous carbon flux resulting from LUC follows the same
526 temporal pattern than the aboveground biomass, as it is simulated as a fixed fraction of aboveground
527 woody mass (sapwood and heartwood) (see Sect. 2.1.5). In S_{age} , for the initial 12 years, the Cohort_6
528 (undisturbed mature forest) is cleared, so that the instantaneous LUC carbon flux is higher than that in
529 S_{ageless} (where the biomass of the single forest patch is “diluted” immediately after the land turnover
530 starts). After that, the instantaneous flux shows a stark drop in S_{age} when the Cohort_3 enters the land



531 turnover. Since then until the end of the simulation, S_{age} has kept a constantly lower instantaneous flux
532 than S_{ageless} because the LUC-perturbed equilibrium biomass in the latter case is higher (Fig. 6a). As a
533 fixed 10% of aboveground woody biomass enters the wood product pool with a 10-year turnover time,
534 delayed carbon emissions from wood products degradation in both simulations are smaller than the
535 instantaneous LUC carbon fluxes. They peak around the 12th year after LUC and remain stable afterwards
536 (Fig. 7a). Overall, S_{age} has a higher LUC-associated direct carbon flux than S_{ageless} for the first 12 years,
537 and a lower one afterwards (Fig. 7a). The cross point for the cumulative LUC-associated direct fluxes
538 equal in S_{age} and S_{ageless} is around the 20th year (Fig. 7b). When summing over the whole simulation period
539 (100 years), the cumulative fluxes by S_{ageless} is lower in S_{age} by about 11 kg C m⁻², or ~110 g C m⁻² yr⁻¹
540 (Fig. 7b) than S_{ageless} .

541 3.1.3 LUC emission and its disaggregation into underlying component carbon fluxes

542 As defined in Eq (4), the net LUC carbon emission (E_{LUC}) is diagnosed as the difference in NBP between
543 the LUC simulation and the control one. Since NBP is further a composite flux determined by carbon
544 uptake and releases (Eq. 3), the difference in $E_{\text{LUC age}}$ and $E_{\text{LUC ageless}}$ can be disaggregated into the effect of
545 each underlying flux, which differs between the LUC simulation and the control simulation. Figure 8
546 presents such disaggregation. All positive values indicate an enhanced carbon uptake or diminished
547 release in the LUC simulation compared to the control one, whereas negative values indicate the reverse
548 cases (i.e., negative values indicate a contribution to enhance E_{LUC}).

549

550 First of all, S_{ageless} (no age dynamics) simulates a larger magnitude (i.e., a larger absolute E_{LUC} value) of
551 mean annual E_{LUC} than S_{age} (with age dynamics), by about 26 g C m⁻² yr⁻¹. Second, for both simulations,
552 the simulated E_{LUC} is an outcome of LUC-associated direct fluxes being compensated for by changes in
553 other fluxes, all of which have an effect to reduce E_{LUC} in this example: NPP, heterotrophic respiration,
554 fire carbon emissions and agricultural harvest.

555

556 NPP is higher in LUC simulations than in the control. This is because young forests are established in the
557 former case (either by merging with existing forest patch or not), leading to a younger leaf age than in the
558 control simulation, which is parameterized to have a higher photosynthetic capacity than older leaves in
559 the model. This suggests the model can somewhat integrate the effect of recovering young forests or
560 intermediate-aged forests with a higher productivity than the old-growth forests, as reported by Tang et al.
561 (2014) using observation data.

562

563 Averaged over the LUC simulation period of 100 years, both S_{age} and S_{ageless} show lower heterotrophic
564 respiration (F_{HR}) than the control. This is because the biomass stock is lower in the LUC simulations



565 (despite a higher NPP, biomass turnover is accelerated due to site perturbation and wood collection in the
566 process of clearing forest for cropland), causing less litter input and less soil carbon stocks (data not
567 shown). The S_{age} simulation shows a much smaller reduction of F_{HR} , mainly because a higher
568 belowground litter is maintained, which results from an abnormally high belowground litter input out of
569 land turnover, driven by a high belowground biomass, as explained in Sect. 3.1.1 (Fig. 6a).

570

571 Decreases in fire carbon emissions (F_{Fire} , from prognostically simulated ‘natural fires’ but not ‘land-
572 clearing fires’) in the LUC simulations in contrast with the control are because the aboveground litter
573 (dominant fuel for fires) is reduced by land turnover. Reductions in fire emissions, and reductions in
574 heterotrophic respiration, are thus driven by the same process, i.e., a reduction in aboveground standing
575 biomass. LUC simulations also result in lower agriculture harvest (F_{AH} , from cropland) although there is
576 no change in the cropland area; this is due to lower biomass in young crop, as the crop harvest is assumed
577 as a constant fraction of the biomass turnover (i.e., routine mortality) at a daily time step. The lower crop
578 biomass in the LUC simulations here is because crop saplings are established on the first day of each
579 calendar year, right before the seasonal biomass peak for the southern hemisphere, which artificially
580 reduces the standing biomass.

581

582 Overall, the lower E_{LUC} magnitude in S_{age} is a result of the lower LUC-associated direct fluxes having
583 been partly compensated for by a higher heterotrophic respiration. The relative magnitudes between E_{LUC}
584 $_{age}$ and $E_{LUC}_{ageless}$ are dominated by these two fluxes, while other fluxes play a less important role.

585 3.2 Simulation over Southern Africa

586 3.2.1 Forest cohort area change as a result of historical land use change

587 One of the useful features of our model development is to account for sub-grid forest age dynamics as a
588 result of historical land use change, as illustrated in Fig. 9 for Southern Africa. When no land use change
589 is included (S_0 , the control simulation), the areas of all forest cohorts are constant over time. Except that
590 younger cohorts have a very small area ($<0.1 \text{ Mkm}^2$) (Cohort₂ and Cohort₃, probably due to improper
591 cohort thresholds on a very small number of grid cells), almost all forests are found in Cohort₆, which
592 represents mature forests. In S_1 where only net land use change is considered, the area of Cohort₆
593 decreases consistently over time due to conversion of forest to other land cover types (Fig. 9a).

594 Occasional increases in areas of other younger cohorts are also present, corresponding to the periods
595 when forest gain happens due to net land use change, for instance, afforestation or reforestation around
596 1700s and in the latter half of the 20th century (Fig. 9a). This is consistent with our rule that forest from
597 abandonment of agriculture is established in the youngest cohort (Fig. 5b – on the right), and progressive



598 movement of forests from younger to older cohorts are also visible as the small waves in the curves of
599 Fig. 9b–f.

600

601 In the S2 simulation with both net land use change and land turnover, large areas of younger forests, in
602 particular of Cohort₁ and Cohort₂, begin to appear as a result of continual creation of forests from land
603 turnover, and subsequent moving of forests from Cohort₁ to Cohort₂. Their temporal changes over time
604 follow those of the forest area subject to land turnover, as shown in Fig. 9a (green dashed line). The area
605 of Cohort₃, however, does not see as much increase as in the two younger cohorts, because forests of
606 Cohort₃ are the primary target for clearance in land turnover and thus are incessantly converted back to
607 (shifting) agriculture. As a result, about half of mature forests (Cohort₆) are left intact from LUC by 2005
608 (Fig. 9h). Most interestingly, when there is a decline in the turnover-impacted area around 1700s (the
609 green arrow in Fig. 9a), a corresponding decline in the area of Cohort₁ is found because these forests
610 move into the next cohort. This pattern of decrease in the current cohort accompanied by the according
611 increase in the next one then propagates into other older cohorts with time, which results in a delayed
612 increase in Cohort₅ around 1750s (Fig. 9g), and finally in Cohort₆ as well (but less prominent because of
613 its already large area). This demonstrates the model feature of older forest recovery in case of decreased
614 land turnover or wood harvest, as explained in Fig. 5b (right hand side). Last, when we further include
615 forest harvest in S3 simulation, because wood harvest area only started to rise in the middle of 20th
616 century, larger areas of Cohort₁ and Cohort₂ cohorts are found compared with S2 in the latter half of the
617 last century, and forest area in Cohort₆ is accordingly lower, being converted to younger cohorts as a
618 result of harvest.

619 3.2.2 Cumulative LUC emissions

620 Cumulative LUC emissions over 1501–2005 in the S_{ageless} and S_{age} simulations for Southern Africa are
621 shown in Fig. 10. In both simulations, including land turnover and wood harvest leads to higher total
622 LUC emissions, by roughly a factor of 1.5 in S_{age} than in the S1 simulation with only net land use change,
623 and by a factor of 2 in S_{ageless}, respectively. Total carbon emissions from all LUC processes in S_{age} are 14.2
624 Pg C, 35% lower than in S_{ageless} (21.9 Pg C). The lower total LUC emissions in S_{age} are mainly due to
625 lower emissions from land turnover, being 6.7 Pg C, almost half of those by S_{ageless} (12.5 Pg C). This is
626 consistent with the findings of idealized grid cell simulation (Sect. 3.1.3).

627

628 Cumulative emissions from net land cover change ($E_{LUC\ net}$) diagnosed from Eq (4) are also lower in S_{age}
629 than in S_{ageless} (6.2 versus 8.4 Pg C) (Fig. 10). This is mainly attributed to a few grid cells, where
630 occasional forest gains (i.e., afforestation or reforestation) occurred during some period over 1501–2005,
631 but eventually, all forests have been cleared. In such cases, occasional forest gains will lead to creation of



632 younger cohorts in the S_{age} simulation; these younger cohorts have lower biomass carbon stock than the
633 otherwise mature forests in the $S_{ageless}$ simulation, hence leading to lower LUC emissions. As for wood
634 harvest, because the area subjected to harvest only started to increase around the middle of the 20th
635 century (Fig. 9), in both S_{age} and $S_{ageless}$ it is mainly mature forests or older cohorts that are harvested,
636 whose biomass density differ little (in the S_{age} simulation, all secondary forests are locked in the
637 continuously expanding land turnover, so the forests subjected to harvest are taken first from older
638 cohorts). As a result, over the region of Southern Africa carbon emissions from wood harvest are almost
639 equal between the two simulations (Fig. 10).

640 **4 Discussion**

641 DGVMs, either used in an off-line mode or coupled with climate models, are powerful tools to investigate
642 the role of past and future land use change in the global carbon cycle perturbed by human activities
643 (Arneth et al., 2017; Le Quéré et al., 2016). Therefore, a more realistic representation of LUC processes
644 in these models is a scientific priority. We included two new features in ORCHIDEE-MICT: gross land
645 use change and forest wood harvest, and sub-grid vegetation cohorts. In a recent review (Prestele et al.,
646 2016), proper representation of gross land use change or sub-grid bi-directional land turnover has been
647 identified as one of the three major challenges in implementing LUC in DGVMs for credible climate
648 assessments. Large underestimation of LUC emissions would occur when gross land use change is
649 ignored, as shown by Wilkenskjeld et al. (2014), Stocker et al. (2014) and also by our results over
650 Southern Africa.

651

652 Shifting cultivation, or forest wood harvest, or more in general forest management, often involves a stable
653 fallow length or rotation cycle, which involves secondary forests rather than primary ones. In tropical
654 regions, fallow lengths in shifting cultivation range from 10 to 40 years (Bruun et al., 2006; Mertz et al.,
655 2008; Thrupp et al., 1997; van Vliet et al., 2012), with a tendency in reduction of fallow length. In Latin
656 American tropics, agricultural abandonment have already led to prominent growth of secondary forests
657 (Chazdon et al., 2016; Poorter et al., 2016). Forest management, including wood harvest, is more
658 common in temperate and boreal regions. In European forests, rotation lengths depend on tree species,
659 regional climate and management purposes (McGrath et al., 2015), ranging from 8–20 years in coppicing
660 systems in southern Europe to 80–120 years in northern countries. The prevalence of secondary forests
661 associated with land use and land use change therefore calls for their representation in DGVMs,
662 especially when modeling land use change. However, to our knowledge, integration of both land use
663 change and sub-grid secondary forests in DGVMs remains rarely reported. Yang et al. (2010) examined
664 the contribution of secondary forests to terrestrial carbon uptake using a vegetation model by explicitly



665 including secondary forest PFTs, but they did not include the dynamic clearing of secondary forests in
666 land use change, nor shifting cultivation. ORCHIDEE-CAN is especially designed to address forest
667 management and species change. Although some certain land use change is included there, but a full LUC
668 scheme addressing all possible LUC processes, including the gross change, is missing (Naudts et al.,
669 2015).

670

671 The gross land use change combined with sub-grid cohorts presented here has shown some promising
672 results. We first confirmed that including gross land use change leads to additional carbon emissions.
673 However, these additional emissions tend to be overestimated when secondary forests are not explicitly
674 accounted for. The idealized grid cell simulation well explained the mechanism driving such
675 overestimation in S_{ageless} simulations at the regional scale. The forest aboveground biomass carbon stocks
676 subjected to LUC impacts, a large part of which are released to the atmosphere as instantaneous fluxes or
677 from later wood product degradation, are likely overestimated when secondary forests are absent in the
678 model. This has given rise to higher LUC emissions in S_{ageless} simulations.

679

680 The results presented here are closely linked with our model parameterization and in particular, various
681 decision rules regarding which forest cohorts to apply for specific LUC processes. In order to examine the
682 influence by including gross land use change, we separated land use change into three LUC processes: net
683 land use change, land turnover and forest wood harvest. Land turnover and secondary forest harvest are
684 parameterized to target intermediate-aged cohorts as a priority. This is the core mechanism driving the
685 lower LUC emissions when sub-grid forest age structure is accounted for. As a preliminary effort to
686 demonstrate the model behaviour, the land turnover parameterization is heavily tied with the input LUC
687 forcing data (LUH1), so that the age of Cohort₃ (as the primary target for land turnover) is set as ~15
688 years, following the assumed mean residence time of shifting cultivation in LUH1 data set (Hurtt et al.,
689 2006). We admit that this parameterization is crucial, because it largely determines the rotation length in
690 the model, and consequently, the amount of carbon stocks subjected to LUC and the difference in
691 estimated LUC emissions between the two model configurations (S_{age} and S_{ageless}). But in fact, because the
692 thresholds in woody mass to distinguish forest cohorts could be configured via a spatial map and such
693 maps could vary among different years, to apply temporally and spatially different turnover lengths is
694 rather straightforward in the model. Such feature is well considered in the model design and could be
695 tested given available forcing LUC data.

696

697 We now discuss some model features as our deliberate decisions and their potential influences in modeled
698 LUC impacts. First, the LUC module developed is intended for usage within DGVMs, and forced with



699 external data sets that provide information on land flows between different land cover types. It is not
700 intended to supersede a land use change model per se, which simulates land use change using other
701 available social and economic information such as population, food demand, wood demand, etc. (Hurtt et
702 al., 2016). In this sense, the LUC module implementation has to inevitably take into account the details of
703 information in forcing data that are available, and to reconcile the potential inconsistency between the
704 model and forcing data. For example, the LUC module presented here can accommodate forest wood
705 harvest from primary and secondary forests when these two sources are distinguished in the forcing data,
706 but hierarchical decision rules are also made when the model and forcing data disagrees (e.g., Fig. 5),
707 such as that prescribed “secondary forest wood harvest” can actually harvest a “primary forest” in the
708 model if all younger cohorts are exhausted.

709

710 Second, because of this clearly defined border of the LUC module to use land areas as the input
711 information, model output from OCHIDEE-MICT can potentially disagree with the socio-economic
712 information used to generate the LUC forcing data. For instance, crop yield simulated by ORCHIDEE
713 may differ with that used to convert food demand/consumption to cropland area, so that simulated crop
714 output or food production will disagree with historical food demand in the real world. The same applies
715 on forestry wood production: simulated harvest wood volume might disagree with the wood volume
716 actually used to generate the harvest area information. This largely raises the issue that, to what extent the
717 information that drives land use change decisions can be *internally* integrated into DGVMs, for example,
718 to use directly crop production, rather than cropland area, or wood volume, rather than forest harvest area
719 as the model input. One potential obstacle is that statistical information (e.g., on wood volume demand) is
720 often available on regional basis (FAO global forest resource assessment, [http://www.fao.org/forest-](http://www.fao.org/forest-resources-assessment/en/)
721 [resources-assessment/en/](http://www.fao.org/forest-resources-assessment/en/); eurostat, <http://ec.europa.eu/eurostat/data/database>), and complex decision rules
722 are needed to disintegrate such information on spatial grids that DGVMs are operated on. But in general,
723 there is need to streamline land use or land management decisions directly into DGVMs. ORCHIDEE-
724 CAN has integrated forest management decisions based on simulated tree diameters and stand density, so
725 that wood volume is actually an output from the model that can be validated against historical statistical
726 data (Naudts et al., 2015).

727

728 The developments presented here mainly build on a model structure to distinguish differently aged
729 cohorts. Nonetheless, we have built a better tool to address the impacts of historical land use change on
730 carbon cycle and climate with these developments. Forest demographic dynamics, which are shown to
731 have great impact on the current northern hemisphere carbon sink (Pan et al., 2011; Piao et al., 2009b),
732 either as a result of active afforestation, or agricultural abandonment or natural regeneration, could then



733 be explicitly investigated. The model also opens the possibility to verify modeled global and regional
734 forest age distribution with that from either forest inventory or satellite imaging. On regional scale such as
735 Europe, it is also possible to account for the LUC impact on full greenhouse gas balance, thanks to the
736 recent developments in pasture module and cropland module (Chang et al., 2015; Wang et al., 2017).

737 **5 Conclusions**

738 We have presented new developments made in a global vegetation model, to include gross land use
739 change and forest wood harvest, in combination with explicit representation of sub-grid forest age
740 dynamics. The results are specific of the ORCHIDEE-MICT model, but the methods are generic for other
741 DGVMs. We demonstrated that over Southern Africa, including gross land use change and forest harvest
742 has led to additional carbon emissions compared to a case where only net transitions are included.
743 However, these additional emissions are overestimated using the traditional approach where secondary
744 forests are not accounted for in the model and quasi-primary forests are cleared for shifting cultivation (or
745 land turnover). We therefore conclude that explicit inclusion of sub-grid secondary forests is crucial for
746 more accurate estimation of land use change emissions. Our developments open the possibility to account
747 for forest demography when evaluating LUC impacts on global carbon cycle and climate.

748 **5 Code availability**

749 The ORCHIDEE-MICT codes used here are a development version deposited on the SVN server:
750 <https://forge.ipsl.jussieu.fr/orchidee/browser/perso/chao.yue/ORCHIDEE-MICT-GLUC> revision 4259
751 from the 20th April 2017. The code is open source, but readers interested in the model application are
752 encouraged to contact the corresponding author.

753 **6 Data availability**

754 Primary data and scripts used in the analysis and other supplementary information that may be useful in
755 reproducing the authors' work can be obtained by contacting the corresponding author.

756 **Acknowledgements**

757 C. Yue and W. Li acknowledge the European Commission-funded project LUC4C (No. 603542). P. Ciais
758 acknowledges the support from the European Research Council through Synergy grant ERC-2013-SyG-
759 610028 "IMBALANCE-P".

760 **References**

761 Arneth, A., Sitch, S., Pongratz, J., Stocker, B. D., Ciais, P., Poulter, B., Bayer, A. D., Bondeau, A., Calle,
762 L., Chini, L. P., Gasser, T., Fader, M., Friedlingstein, P., Kato, E., Li, W., Lindeskog, M., Nabel, J. E. M.
763 S., Pugh, T. a. M., Robertson, E., Viovy, N., Yue, C. and Zaehle, S.: Historical carbon dioxide emissions
764 caused by land-use changes are possibly larger than assumed, *Nat. Geosci.*, 10(2), 79–84,
765 doi:10.1038/ngeo2882, 2017.



- 766 Bruun, T. B., Mertz, O. and Elberling, B.: Linking yields of upland rice in shifting cultivation to fallow
767 length and soil properties, *Agric. Ecosyst. Environ.*, 113(1–4), 139–149, doi:10.1016/j.agee.2005.09.012,
768 2006.
- 769 Chang, J., Ciais, P., Viovy, N., Vuichard, N., Sultan, B. and Soussana, J.-F.: The greenhouse gas balance
770 of European grasslands, *Glob. Change Biol.*, 21(10), 3748–3761, doi:10.1111/gcb.12998, 2015.
- 771 Chang, J. F., Viovy, N., Vuichard, N., Ciais, P., Wang, T., Cozic, A., Lardy, R., Graux, A.-I., Klumpp,
772 K., Martin, R. and Soussana, J.-F.: Incorporating grassland management in ORCHIDEE: model
773 description and evaluation at 11 eddy-covariance sites in Europe, *Geosci Model Dev.*, 6(6), 2165–2181,
774 doi:10.5194/gmd-6-2165-2013, 2013.
- 775 Chazdon, R. L., Broadbent, E. N., Rozendaal, D. M. A., Bongers, F., Zambrano, A. M. A., Aide, T. M.,
776 Balvanera, P., Becknell, J. M., Boukili, V., Brancalion, P. H. S., Craven, D., Almeida-Cortez, J. S.,
777 Cabral, G. A. L., Jong, B. de, Denslow, J. S., Dent, D. H., DeWalt, S. J., Dupuy, J. M., Durán, S. M.,
778 Espirito-Santo, M. M., Fandino, M. C., César, R. G., Hall, J. S., Hernández-Stefanoni, J. L., Jakovac, C.
779 C., Junqueira, A. B., Kennard, D., Letcher, S. G., Lohbeck, M., Martínez-Ramos, M., Massoca, P.,
780 Meave, J. A., Mesquita, R., Mora, F., Muñoz, R., Muscarella, R., Nunes, Y. R. F., Ochoa-Gaona, S.,
781 Orihuela-Belmonte, E., Peña-Claros, M., Pérez-García, E. A., Piotta, D., Powers, J. S., Rodríguez-
782 Velazquez, J., Romero-Pérez, I. E., Ruiz, J., Saldarriaga, J. G., Sanchez-Azofeifa, A., Schwartz, N. B.,
783 Steininger, M. K., Swenson, N. G., Uriarte, M., Breugel, M. van, Wal, H. van der, Veloso, M. D. M.,
784 Vester, H., Vieira, I. C. G., Bentos, T. V., Williamson, G. B. and Poorter, L.: Carbon sequestration
785 potential of second-growth forest regeneration in the Latin American tropics, *Sci. Adv.*, 2(5), e1501639,
786 doi:10.1126/sciadv.1501639, 2016.
- 787 Don, A., Schumacher, J. and Freibauer, A.: Impact of tropical land-use change on soil organic carbon
788 stocks – a meta-analysis, *Glob. Change Biol.*, 17(4), 1658–1670, doi:10.1111/j.1365-2486.2010.02336.x,
789 2011.
- 790 Foley, J. A., DeFries, R., Asner, G. P., Barford, C., Bonan, G., Carpenter, S. R., Chapin, F. S., Coe, M. T.,
791 Daily, G. C., Gibbs, H. K., Helkowski, J. H., Holloway, T., Howard, E. A., Kucharik, C. J., Monfreda, C.,
792 Patz, J. A., Prentice, I. C., Ramankutty, N. and Snyder, P. K.: Global Consequences of Land Use,
793 *Science*, 309(5734), 570–574, doi:10.1126/science.1111772, 2005.
- 794 Guo, L. B. and Gifford, R. M.: Soil carbon stocks and land use change: a meta analysis, *Glob. Change*
795 *Biol.*, 8, 345–360, 2002.
- 796 Houghton, R. A.: The annual net flux of carbon to the atmosphere from changes in land use 1850–1990*,
797 *Tellus B*, 51(2), 298–313, doi:10.1034/j.1600-0889.1999.00013.x, 1999.
- 798 Houghton, R. A., House, J. I., Pongratz, J., van der Werf, G. R., DeFries, R. S., Hansen, M. C., Le Quéré,
799 C. and Ramankutty, N.: Carbon emissions from land use and land-cover change, *Biogeosciences*, 9(12),
800 5125–5142, doi:10.5194/bg-9-5125-2012, 2012.
- 801 Hurtt, G. C., Frohking, S., Fearon, M. G., Moore, B., Shevliakova, E., Malyshev, S., Pacala, S. W. and
802 Houghton, R. A.: The underpinnings of land-use history: three centuries of global gridded land-use
803 transitions, wood-harvest activity, and resulting secondary lands, *Glob. Change Biol.*, 12(7), 1208–1229,
804 doi:10.1111/j.1365-2486.2006.01150.x, 2006.
- 805 Hurtt, G. C., Chini, L. P., Frohking, S., Betts, R. A., Feddema, J., Fischer, G., Fisk, J. P., Hibbard, K.,
806 Houghton, R. A., Janetos, A., Jones, C. D., Kindermann, G., Kinoshita, T., Goldewijk, K. K., Riahi, K.,



- 807 Shevliakova, E., Smith, S., Stehfest, E., Thomson, A., Thornton, P., Vuuren, D. P. van and Wang, Y. P.:
808 Harmonization of land-use scenarios for the period 1500–2100: 600 years of global gridded annual land-
809 use transitions, wood harvest, and resulting secondary lands, *Clim. Change*, 109(1–2), 117,
810 doi:10.1007/s10584-011-0153-2, 2011.
- 811 Krinner, G., Viovy, N., de Noblet-Ducoudré, N., Ogée, J., Polcher, J., Friedlingstein, P., Ciais, P., Sitch,
812 S. and Prentice, I. C.: A dynamic global vegetation model for studies of the coupled atmosphere-
813 biosphere system, *Glob. Biogeochem. Cycles*, 19(1), GB1015, doi:10.1029/2003GB002199, 2005.
- 814 Lanly, J. P.: Defining and measuring shifting cultivation, Unasylva FAO [online] Available from:
815 <http://agris.fao.org/agris-search/search.do?recordID=XF8552163> (Accessed 14 May 2017), 1985.
- 816 Le Quéré, C., Andrew, R. M., Canadell, J. G., Sitch, S., Korsbakken, J. I., Peters, G. P., Manning, A. C.,
817 Boden, T. A., Tans, P. P., Houghton, R. A., Keeling, R. F., Alin, S., Andrews, O. D., Anthoni, P.,
818 Barbero, L., Bopp, L., Chevallier, F., Chini, L. P., Ciais, P., Currie, K., Delire, C., Doney, S. C.,
819 Friedlingstein, P., Gkritzalis, T., Harris, I., Hauck, J., Haverd, V., Hoppema, M., Klein Goldewijk, K.,
820 Jain, A. K., Kato, E., Körtzinger, A., Landschützer, P., Lefèvre, N., Lenton, A., Lienert, S., Lombardozi,
821 D., Melton, J. R., Metzl, N., Millero, F., Monteiro, P. M. S., Munro, D. R., Nabel, J. E. M. S., Nakaoka,
822 S.-I., O'Brien, K., Olsen, A., Omar, A. M., Ono, T., Pierrot, D., Poulter, B., Rödenbeck, C., Salisbury, J.,
823 Schuster, U., Schwinger, J., Séférian, R., Skjelvan, I., Stocker, B. D., Sutton, A. J., Takahashi, T., Tian,
824 H., Tilbrook, B., van der Laan-Luijkx, I. T., van der Werf, G. R., Viovy, N., Walker, A. P., Wiltshire, A.
825 J., and Zaehle, S.: Global Carbon Budget 2016, *Earth Syst. Sci. Data*, 8, 605–649, doi:10.5194/essd-8-
826 605-2016, 2016.
- 827 Li W., Ciais P., Peng S.S., Yue C., Wang Y.L., Thurner M., Saatchi S., Arneeth A., Avitabile V.,
828 Carvalhais N., Harper A., Kato E., Koven C., Liu Y.Y., Nabel J., Pan Y.D., Pongratz J., Poulter B., Pugh
829 T., Santoro M., Sitch S., Stocker B.D., Viovy N., Wiltshire A., Yousefpour R., and Zaehle S. Land-use
830 and land-cover change carbon emissions between 1901 and 2012 constrained by biomass observations.
831 Submitted to Biogeosciences.
- 832 Luyssaert, S., Janssens, I., Stoy, P. C., Estel, S., Pongratz, J., Ceschia, E., Churkina, G., Don, A., Erb, K.,
833 Ferlicoq, M., Gielen, B., Grünwald, T., Houghton, R. A., Klumpp, K., Knohl, A., Kolb, T., Kuehnerle,
834 T., Laurila, T., Lohila, A., Loustau, D., McGrath, M. J., Meyfroidt, P., Moors, E. J., Naudts, K., Novick,
835 K., Otto, J., Pilegaard, K., Pio, C. A., Rambal, S., Rebmann, C., Ryder, J., Suyker, A. E., Varlagin, A.,
836 Wattenbach, M. and Dolman, A. J.: Land management and land-cover change have impacts of similar
837 magnitude on surface temperature, *Nat. Clim. Change*, 4(5), 389–393, doi:10.1038/nclimate2196, 2014.
- 838 Mahmood, R., Pielke, R. A., Hubbard, K. G., Niyogi, D., Dirmeyer, P. A., McAlpine, C., Carleton, A. M.,
839 Hale, R., Gameda, S., Beltrán-Przekurat, A., Baker, B., McNider, R., Legates, D. R., Shepherd, M., Du,
840 J., Blanken, P. D., Frauenfeld, O. W., Nair, U. S. and Fall, S.: Land cover changes and their
841 biogeophysical effects on climate, *Int. J. Climatol.*, 34(4), 929–953, doi:10.1002/joc.3736, 2014.
- 842 Mason Earles, J., Yeh, S. and Skog, K. E.: Timing of carbon emissions from global forest clearance, *Nat.*
843 *Clim. Change*, 2(9), 682–685, doi:10.1038/nclimate1535, 2012.
- 844 McGrath, M. J., Luyssaert, S., Meyfroidt, P., Kaplan, J. O., Bürgi, M., Chen, Y., Erb, K., Gimmi, U.,
845 McInerney, D., Naudts, K., Otto, J., Pasztor, F., Ryder, J., Schelhaas, M.-J. and Valade, A.:
846 Reconstructing European forest management from 1600 to 2010, *Biogeosciences*, 12(14), 4291–4316,
847 doi:10.5194/bg-12-4291-2015, 2015.



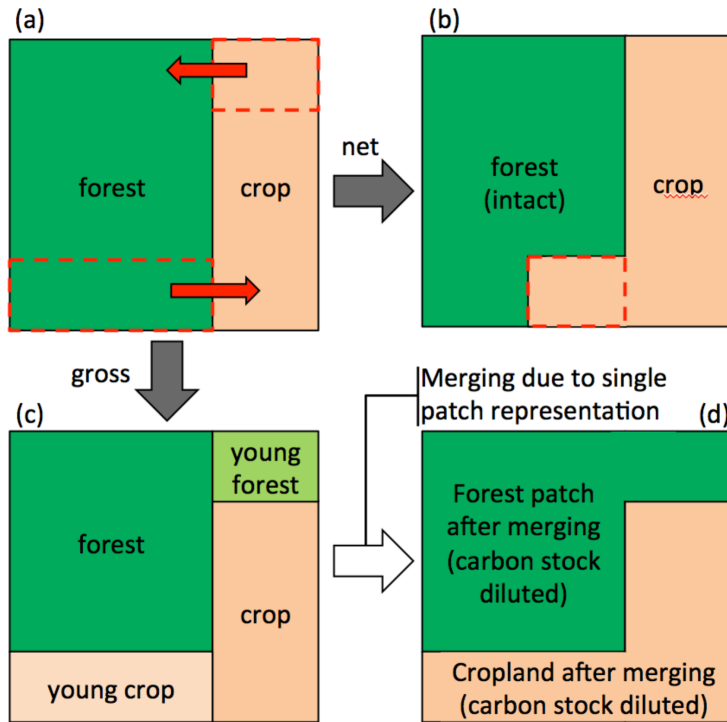
- 848 Mertz, O., Wadley, R. L., Nielsen, U., Bruun, T. B., Colfer, C. J. P., de Neergaard, A., Jepsen, M. R.,
849 Martinussen, T., Zhao, Q., Noweg, G. T. and Magid, J.: A fresh look at shifting cultivation: Fallow length
850 an uncertain indicator of productivity, *Agric. Syst.*, 96(1–3), 75–84, doi:10.1016/j.agsy.2007.06.002,
851 2008.
- 852 Morton, D. C., Defries, R. S., Randerson, J. T., Giglio, L., Schroeder, W. and Van Der Werf, G. R.:
853 Agricultural intensification increases deforestation fire activity in Amazonia, *Glob. Change Biol.*, 14(10),
854 2262–2275, doi:10.1111/j.1365-2486.2008.01652.x, 2008.
- 855 Naudts, K., Ryder, J., McGrath, M. J., Otto, J., Chen, Y., Valade, A., Bellasen, V., Berhongaray, G.,
856 Bönisch, G., Campioli, M., Ghattas, J., De Groote, T., Haverd, V., Kattge, J., MacBean, N., Maignan, F.,
857 Merilä, P., Penuelas, J., Peylin, P., Pinty, B., Pretzsch, H., Schulze, E. D., Solyga, D., Vuichard, N., Yan,
858 Y. and Luysaert, S.: A vertically discretised canopy description for ORCHIDEE (SVN r2290) and the
859 modifications to the energy, water and carbon fluxes, *Geosci Model Dev.*, 8(7), 2035–2065,
860 doi:10.5194/gmd-8-2035-2015, 2015.
- 861 Pan, Y., Birdsey, R. A., Fang, J., Houghton, R., Kauppi, P. E., Kurz, W. A., Phillips, O. L., Shvidenko,
862 A., Lewis, S. L., Canadell, J. G., Ciais, P., Jackson, R. B., Pacala, S. W., McGuire, A. D., Piao, S.,
863 Rautiainen, A., Sitch, S. and Hayes, D.: A Large and Persistent Carbon Sink in the World's Forests,
864 *Science*, 333(6045), 988–993, doi:10.1126/science.1201609, 2011.
- 865 Piao, S., Ciais, P., Friedlingstein, P., de Noblet-Ducoudré, N., Cadule, P., Viovy, N. and Wang, T.:
866 Spatiotemporal patterns of terrestrial carbon cycle during the 20th century, *Glob. Biogeochem. Cycles*,
867 23(4), GB4026, doi:10.1029/2008GB003339, 2009a.
- 868 Piao, S., Fang, J., Ciais, P., Peylin, P., Huang, Y., Sitch, S. and Wang, T.: The carbon balance of
869 terrestrial ecosystems in China, *Nature*, 458(7241), 1009–1013, doi:10.1038/nature07944, 2009b.
- 870 Poeplau, C., Don, A., Vesterdal, L., Leifeld, J., Van Wesemael, B., Schumacher, J. and Gensior, A.:
871 Temporal dynamics of soil organic carbon after land-use change in the temperate zone – carbon response
872 functions as a model approach, *Glob. Change Biol.*, 17(7), 2415–2427, doi:10.1111/j.1365-
873 2486.2011.02408.x, 2011.
- 874 Pongratz, J., Reick, C. H., Houghton, R. A. and House, J. I.: Terminology as a key uncertainty in net land
875 use and land cover change carbon flux estimates, *Earth Syst Dynam.*, 5(1), 177–195, doi:10.5194/esd-5-
876 177-2014, 2014.
- 877 Poorter, L., Bongers, F., Aide, T. M., Almeyda Zambrano, A. M., Balvanera, P., Becknell, J. M., Boukili,
878 V., Brancalion, P. H. S., Broadbent, E. N., Chazdon, R. L., Craven, D., de Almeida-Cortez, J. S., Cabral,
879 G. A. L., de Jong, B. H. J., Denslow, J. S., Dent, D. H., DeWalt, S. J., Dupuy, J. M., Durán, S. M.,
880 Espirito-Santo, M. M., Fandino, M. C., César, R. G., Hall, J. S., Hernandez-Stefanoni, J. L., Jakovac, C.
881 C., Junqueira, A. B., Kennard, D., Letcher, S. G., Licona, J.-C., Lohbeck, M., Marín-Spiotta, E.,
882 Martínez-Ramos, M., Massoca, P., Meave, J. A., Mesquita, R., Mora, F., Muñoz, R., Muscarella, R.,
883 Nunes, Y. R. F., Ochoa-Gaona, S., de Oliveira, A. A., Orihuela-Belmonte, E., Peña-Claros, M., Pérez-
884 García, E. A., Piotta, D., Powers, J. S., Rodríguez-Velázquez, J., Romero-Pérez, I. E., Ruiz, J.,
885 Saldarriaga, J. G., Sanchez-Azofeifa, A., Schwartz, N. B., Steininger, M. K., Swenson, N. G., Toledo, M.,
886 Uriarte, M., van Breugel, M., van der Wal, H., Veloso, M. D. M., Vester, H. F. M., Vicentini, A., Vieira,
887 I. C. G., Bentos, T. V., Williamson, G. B. and Rozendaal, D. M. A.: Biomass resilience of Neotropical
888 secondary forests, *Nature*, 530(7589), 211–214, doi:10.1038/nature16512, 2016.



- 889 Powers, J. S., Corre, M. D., Twine, T. E. and Veldkamp, E.: Geographic bias of field observations of soil
890 carbon stocks with tropical land-use changes precludes spatial extrapolation, *Proc. Natl. Acad. Sci.*,
891 108(15), 6318–6322, doi:10.1073/pnas.1016774108, 2011.
- 892 Prestele, R., Arneth, A., Bondeau, A., de Noblet-Ducoudré, N., Pugh, T. A. M., Sitch, S., Stehfest, E. and
893 Verburg, P. H.: Current challenges of implementing land-use and land-cover change in climate
894 assessments, *Earth Syst Dynam Discuss*, 2016, 1–28, doi:10.5194/esd-2016-39, 2016.
- 895 Sitch, S., Friedlingstein, P., Gruber, N., Jones, S. D., Murray-Tortarolo, G., Ahlström, A., Doney, S. C.,
896 Graven, H., Heinze, C., Huntingford, C. and others: Recent trends and drivers of regional sources and
897 sinks of carbon dioxide, *Biogeosciences*, 12(3), 653–679, 2015.
- 898 Stocker, B. D., Feissli, F., Strassmann, K. M., Spahni, R. and Joos, F.: Past and future carbon fluxes from
899 land use change, shifting cultivation and wood harvest, *Tellus B*, 66(0), doi:10.3402/tellusb.v66.23188,
900 2014.
- 901 Thrupp, L. A., Hecht, S. and Browder, J. O.: diversity and dynamics of shifting cultivation, [online]
902 Available from: <http://agris.fao.org/agris-search/search.do?recordID=US201300022402> (Accessed 11
903 May 2017), 1997.
- 904 van Vliet, N., Mertz, O., Heinemann, A., Langanke, T., Pascual, U., Schmook, B., Adams, C., Schmidt-
905 Vogt, D., Messerli, P., Leisz, S., Castella, J.-C., Jørgensen, L., Birch-Thomsen, T., Hett, C., Bech-Bruun,
906 T., Ickowitz, A., Vu, K. C., Yasuyuki, K., Fox, J., Padoch, C., Dressler, W. and Ziegler, A. D.: Trends,
907 drivers and impacts of changes in swidden cultivation in tropical forest-agriculture frontiers: A global
908 assessment, *Glob. Environ. Change*, 22(2), 418–429, doi:10.1016/j.gloenvcha.2011.10.009, 2012.
- 909 Wang, X., Ciais, P., Li, L., Ruget, F., Vuichard, N., Viovy, N., Zhou, F., Chang, J., Wu, X., Zhao, H. and
910 Piao, S.: Management outweighs climate change on affecting length of rice growing period for early rice
911 and single rice in China during 1991–2012, *Agric. For. Meteorol.*, 233, 1–11,
912 doi:10.1016/j.agrformet.2016.10.016, 2017.
- 913 Wilkenskjeld, S., Kloster, S., Pongratz, J., Raddatz, T. and Reick, C. H.: Comparing the influence of net
914 and gross anthropogenic land-use and land-cover changes on the carbon cycle in the MPI-ESM,
915 *Biogeosciences*, 11(17), 4817–4828, doi:10.5194/bg-11-4817-2014, 2014.
- 916 Yang, X., Richardson, T. K. and Jain, A. K.: Contributions of secondary forest and nitrogen dynamics to
917 terrestrial carbon uptake, *Biogeosciences*, 7(10), 3041–3050, doi:10.5194/bg-7-3041-2010, 2010.
- 918 Yue, C., Ciais, P., Cadule, P., Thonicke, K., Archibald, S., Poulter, B., Hao, W. M., Hantson, S.,
919 Mouillot, F., Friedlingstein, P., Maignan, F. and Viovy, N.: Modelling the role of fires in the terrestrial
920 carbon balance by incorporating SPITFIRE into the global vegetation model ORCHIDEE – Part 1:
921 simulating historical global burned area and fire regimes, *Geosci. Model Dev.*, 7(6), 2747–2767,
922 doi:10.5194/gmd-7-2747-2014, 2014.
- 923



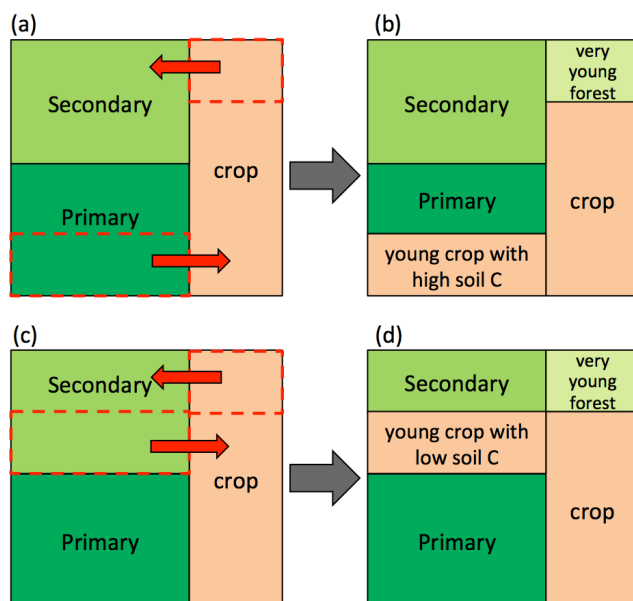
924 **Figures and Tables**



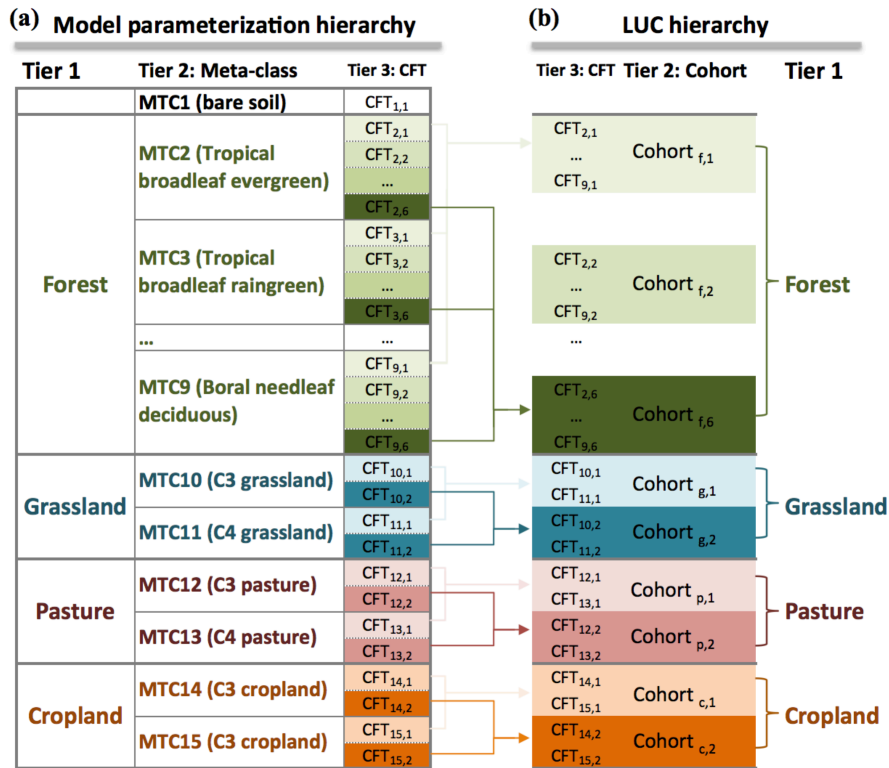
925
 926 Fig. 1 Schematic illustration of gross versus net land use change, with each land cover type being
 927 represented using a single patch within a model grid cell. The figure is adapted from Stocker et al. (2014).
 928 (a) Original fractions of forest and cropland and land use transitions. Dashed red rectangles indicate areas
 929 subject to LUC and red arrows indicate land flow direction. Here LUC consists of a net loss in forest and
 930 a simultaneous bi-directional flow between forest and cropland. (b) Post-LUC fractions of forest and
 931 cropland following the original LUC scheme of net transition only in ORCHIDEE. Bi-directional land
 932 flow is omitted, with only cropland area being expanded to account for the net increase (as a result of the
 933 net forest loss, as indicated by the dashed red rectangle). The soil carbon stock of the new cropland patch
 934 is an area-weighted mean between that of the original cropland, and the legacy stock from the former
 935 forest. Carbon stock of the remaining forest patch is left intact. (c) Intermediate post-LUC land cover
 936 pattern after accounting for gross transition. Both the net loss of forest and bi-directional land flows are
 937 accounted for, with two young patches of forest and cropland being established, respectively. (d) Final
 938 state of post-LUC land cover after accounting for gross LUC with no sub-grid cohorts. The carbon stocks
 939 of the remaining (original) forest and the newly created forest are immediately merged following LUC



940 because there are no sub-grid cohorts. The same applies for cropland as well. Note that although forest
941 and cropland fractions are ultimately the same as in (b), the carbon densities are different.
942
943
944



945
946 Fig. 2 Gross land use change involving forests with different ages, under a model scheme capable of
947 representing sub-grid vegetation cohorts. The figure is adapted from Stocker et al. (2014). LUC here is
948 similar as in Fig. 1, except that forest is no longer a single ageless patch but consists of two patches of
949 primary and secondary forests, i.e., having an age structure. (a) The same area of forest is converted to
950 cropland as in Fig. 1a but conversion is made from primary forest. (b) Consequently, a ‘young’ cropland
951 patch with rich legacy forest soil C is established. In the meanwhile, a very young forest patch is
952 established due to the bi-directional gross land flux. Because the model uses multiple sub-grid patches to
953 represent vegetation age structure (or differently aged cohorts), merging of patches with different carbon
954 stocks is no longer necessary. Subplot (c) shows an alternative to (a) where conversion of forest to
955 cropland is made on a secondary forest. Correspondingly, in subplot (d), which shows the post-LUC state
956 of (c), the established young cropland patch will have lower legacy soil C than that in (b).
957



958

959

960

961

962

963

964

965

966

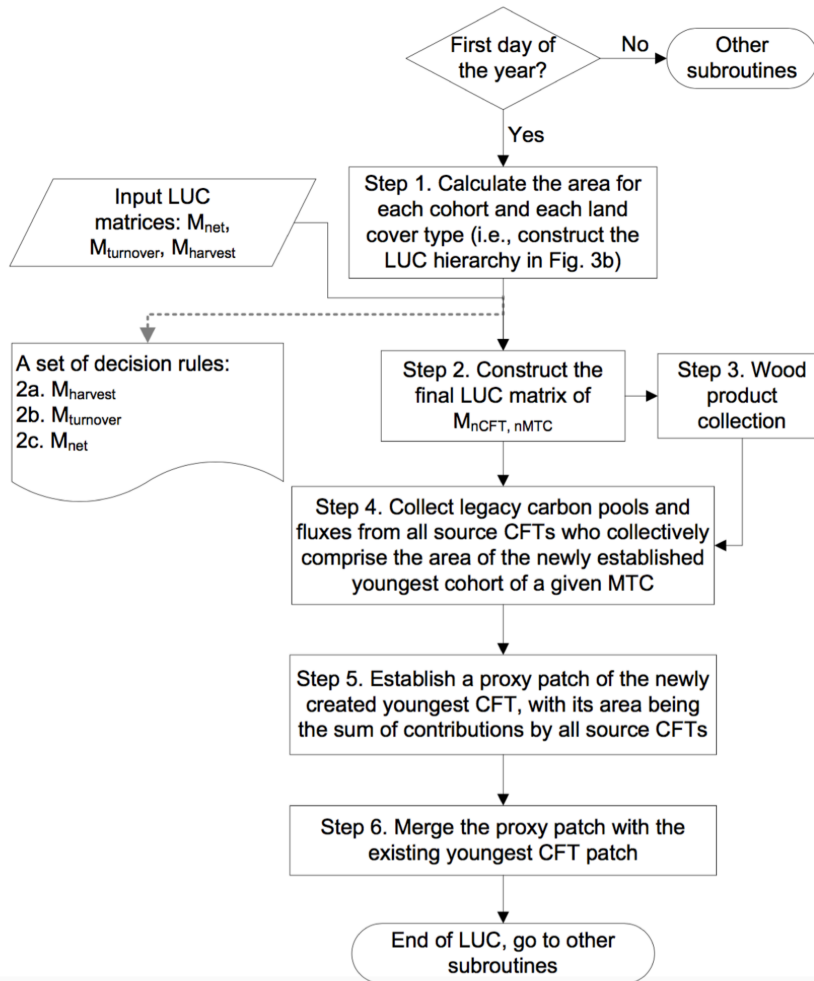
967

968

969

970

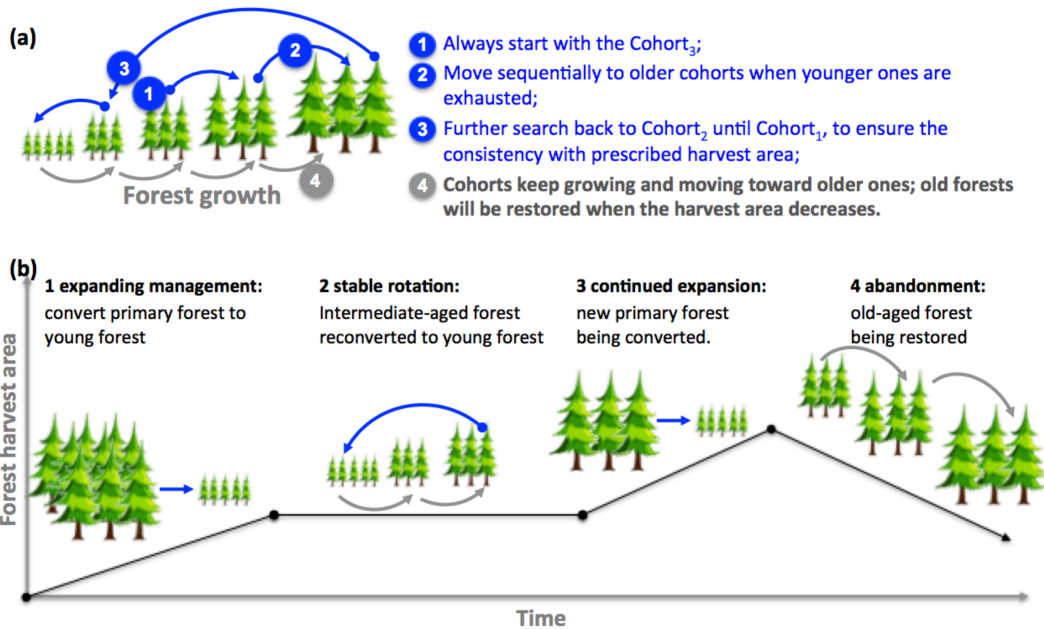
Fig. 3 Two parallel hierarchies from the model parameterization and land use change perspective. (a) Sub-grid cohort function types (CFTs) as inheritances of meta-classes (MTCs) and the corresponding parameterization hierarchy. There are in total 14 vegetative MTCs corresponding to four vegetation types. The notation of CFT_{i,j} indicates that it inherits from MTC_i and belongs to the jth cohort (Cohort_j). Each forest MTC has six cohorts, with Cohort₁ being the youngest and Cohort₆ the oldest, whereas each herbaceous MTC is set tentatively to have two cohorts. Darker colors indicate older cohorts. (b) Within the gross LUC module hierarchy, Tier 3 remains the level of CFT, but CFTs are re-organized to derive the Tier 2 information based on the level of cohorts, under the same Tier 1 as in (a). A cohort bearing the notation of Cohort_{v,i} indicates it belongs to vegetation type 'v' (where 'v' could be forest, natural grassland, pasture and cropland) and meta-class 'i'. This re-organization of the hierarchy is to prepare for properly allocating prescribed LUC transitions first onto the cohort level, then further to different CFTs within each cohort.



971

972 Fig. 4 Schematic representation of the new LUC scheme in ORCHIDEE-MICT accounting for net land

973 use change, land turnover and forest harvest in combination with sub-grid cohort representation.



974

975 Fig. 5 Rules of selection of forest cohorts in the wood harvest to account for dynamic changes in the area

976 subjected to wood harvest over time. (a) Rule for the selection of forest cohort (blue arrows). Clear-cut

977 harvest (1) first starts with intermediate-aged cohort, then moves to older cohorts until the oldest one; (2)

978 if the prescribed harvested area still cannot be satisfied, then the selection will move back to the even

979 younger cohorts (3) until the youngest one until the prescribed harvested area is fulfilled. Independent of

980 the harvest activity is the movement of forests from younger cohorts to older ones because of growth

981 (gray arrows). (b) Example of cohort dynamics for changes in the harvest area over time shown in the

982 black curve: (1) before the onset of any harvest activity (i.e., after the model spin-up), only the oldest

983 cohorts are available so harvest starts with the primary forest; (2) for a stable harvest area, a steady-state

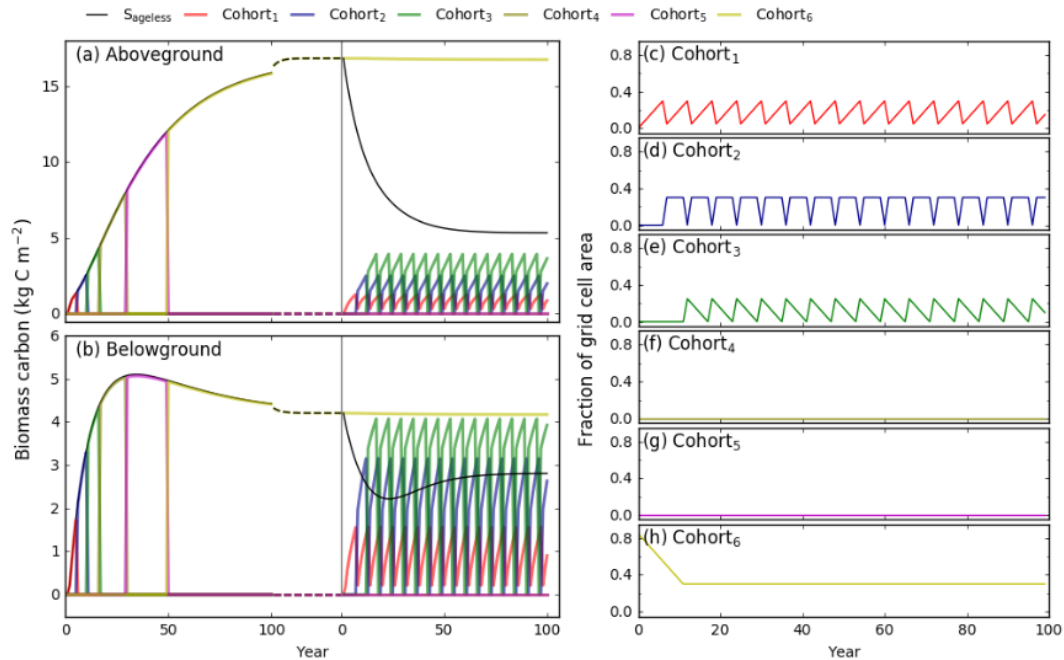
984 cycle is established involving only secondary forest (intermediate secondary cohorts being harvested

985 represented by the blue arrow, and younger cohorts growing represented by gray arrows); (3) then with an

986 increase in harvest area, more primary forests are harvested; (4) finally in this example, the harvest area

987 decreases, and older cohorts are restored.

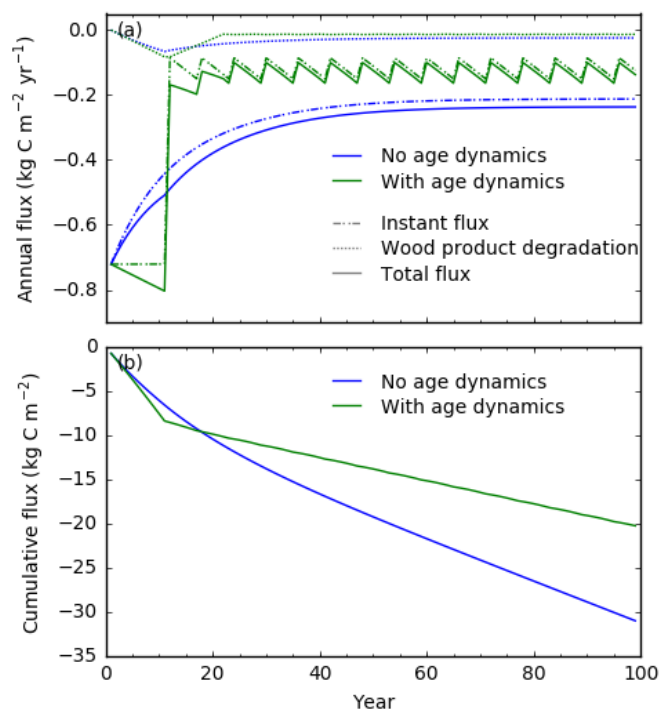
988



989

990 Fig. 6 Biomass carbon stock as simulated by two model configurations without ($S_{ageless}$) and with sub-grid
 991 age dynamics for (a) aboveground biomass and (b) belowground biomass. Data shown are the biomass
 992 accumulation during the spin-up simulation (which lasts for 450 years, from Year 0 until the end of
 993 dashed line) and transient simulation (which lasts for 100 years) where an annual forest-cropland turnover
 994 with 5% of the grid cell area is applied. Vertical gray lines indicate the end of the spin-up and start of
 995 transient simulations. Subplot (c)–(h) show ground coverage by different forest cohorts as fractions of
 996 grid cell during the transient simulation only.

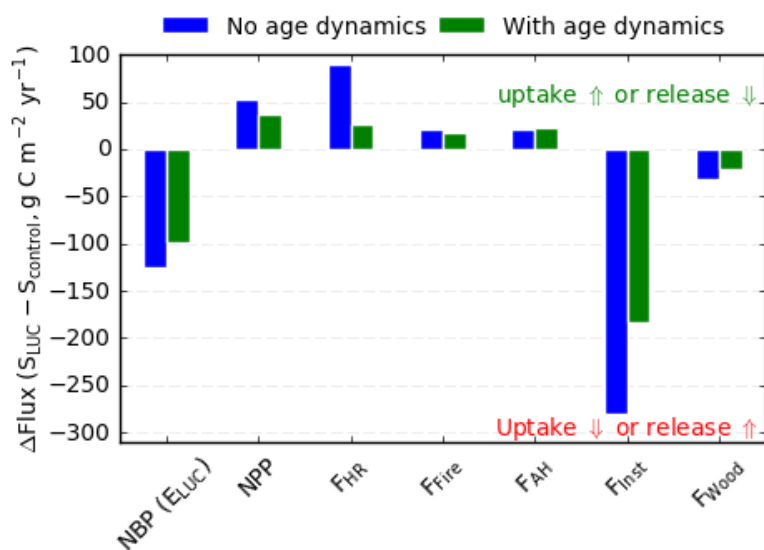
997



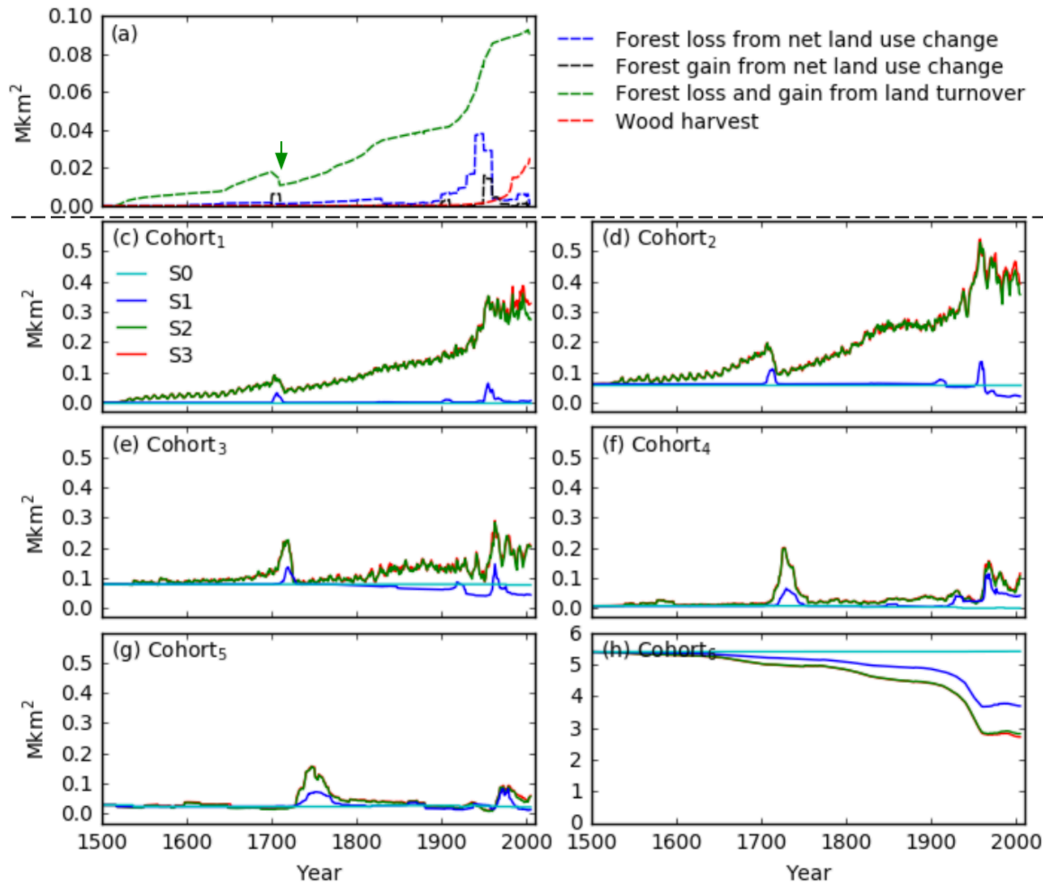
998

999 Fig. 7 (a) Carbon fluxes directly associated with LUC (negative values for carbon lost from ecosystems):
1000 instantaneous flux (dash-dotted line), flux from wood products degradation (dotted line) and the total flux
1001 (solid line) for simulations with (green) and without (blue) sub-grid age dynamics. (b) Cumulative LUC-
1002 associated direct fluxes (the sum of instantaneous and wood products degradation fluxes) for simulations
1003 with (green) and without (blue) sub-grid age dynamics. Data are shown for an annual forest-cropland
1004 turnover of 5% of the grid cell area for 100 years.

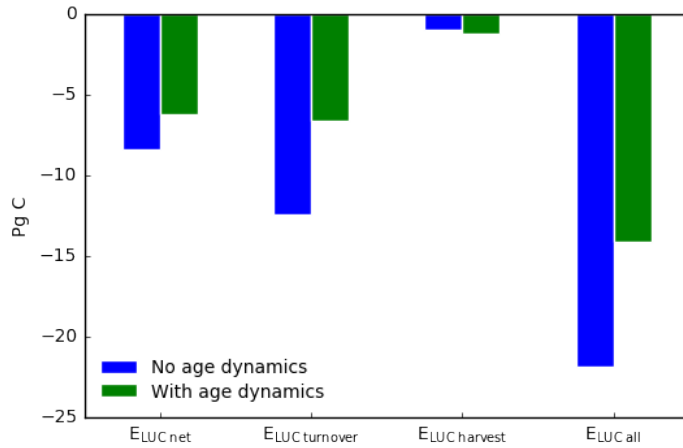
1005



1006
 1007 Fig. 8 Mean annual carbon flux differences between the LUC and control simulations over 100 years for
 1008 an annual forest-cropland turnover with 5% of the grid cell area for two model configurations: without
 1009 (blue) and with sub-grid age dynamics (green). Positive (negative) values indicate contributions to
 1010 enhanced carbon sink (source) in LUC simulation compared to the control one, either by stronger
 1011 (weaker) carbon uptake or smaller (stronger) carbon release. E_{LUC} is shown as a negative value here, i.e.,
 1012 the LUC simulation has a lower NBP than the control one, indicating an effect of net carbon source by
 1013 LUC.



1014
 1015 Fig. 9 Areas subject to historical land use change and the resulting modeled temporal changes in areas of
 1016 different forest cohorts in Southern Africa. (a) Areas subjected to historical land use change in which
 1017 forests are involved. Data are from LUH1 reconstruction (Hurtt et al., 2011) after adaption for
 1018 ORCHIDEE-MICT. Three types of LUC activities are shown and their effects elucidated by factorial
 1019 simulations (Table 2). These are: forest loss (blue dashed line) and gain (black dashed line) resulting from
 1020 net land use change, forest involved in land turnover (both loss and gain in equal amount, green dashed
 1021 line), and forest area subjected to wood harvest (red dashed line). (b)–(h) Areas of forest cohorts (Cohort₁
 1022 = the youngest, Cohort₆ = the oldest) for four factorial simulations (Table 2) where no land use change
 1023 occurs in S0, and the three LUC types are added in a factorial set-up in S1 (net land use change, blue solid
 1024 line), S2 (net land use change + land turnover, green solid line) and S3 (net land use change + land
 1025 turnover + wood harvest, red solid line). Note y-scale values in subplot (a) and (h) differ from others.
 1026



1027
 1028 Fig. 10 Cumulative carbon emissions over 1501-2005 from land use change over the region of South
 1029 Africa from three LUC processes: net land use change ($E_{LUC\ net}$), land turnover ($E_{LUC\ turnover}$) and wood
 1030 harvest ($E_{LUC\ harvest}$) and the sum of them ($E_{LUC\ all}$), for two model configurations: with (S_{age} , green color)
 1031 and without ($S_{ageless}$, blue color) sub-grid age dynamics.

1032
 1033

1034 Table 1. Fractions of aboveground woody biomass lost immediately to the atmosphere during a forest
 1035 clearing, and channeled to 10-year and 100-year turnover wood product pools. These fractions are
 1036 different depending on forest biomes.

	Tropical forest	Temperate forest	Boreal forest
$F_{instant}$	0.897	0.597	0.597
F_{10yr}	0.103	0.299	0.299
F_{100yr}	0	0.104	0.104

1037
 1038
 1039

1040 Table 2 Factorial simulations to separate contributions from each of the three LUC processes: net land use
 1041 change ($E_{LUC\ net}$), land turnover ($E_{LUC\ turnover}$) and wood harvest ($E_{LUC\ harvest}$). The plus signs (“+”) indicate
 1042 that the corresponding processes (matrices) are included in the simulations, with $S_{0\ age}$ ($S_{0\ ageless}$) having no
 1043 LUC activities to $S_{3\ age}$ ($S_{3\ ageless}$) including all LUC processes. The land use carbon emissions are
 1044 quantified as the difference in NBP between simulations with and without LUC or a specific LUC process
 1045 (Eq. 4).



Simulations and LUC processes included

Simulations	Net land use change	Land turnover	Wood harvest
$S0_{age}, S0_{ageless}$			
$S1_{age}, S1_{ageless}$	+		
$S2_{age}, S2_{ageless}$	+	+	
$S3_{age}, S3_{ageless}$	+	+	+

Diagnostic of LUC emissions

Without age dynamics	With age dynamics
$E_{LUC\ net, ageless} = NBP_{S1_{ageless}} - NBP_{S0_{ageless}}$	$E_{LUC\ net, age} = NBP_{S1_{age}} - NBP_{S0_{age}}$
$E_{LUC\ turnover, ageless} = NBP_{S2_{ageless}} - NBP_{S1_{ageless}}$	$E_{LUC\ turnover, age} = NBP_{S2_{age}} - NBP_{S1_{age}}$
$E_{LUC\ harvest, ageless} = NBP_{S3_{ageless}} - NBP_{S2_{ageless}}$	$E_{LUC\ harvest, age} = NBP_{S3_{age}} - NBP_{S2_{age}}$

1046